American Mineralogist, Volume 77, pages 1206–1222, 1992

# The fluid-absent melting of phlogopite + quartz: Experiments and models

**Daniel Vielzeuf**
Département de Géologie, CNRS-URA 10, 5 rue Kessler, 63038 Clermont-Ferrand, France
**John D. Clemens**
Department of Geology, University of Manchester, M13 9PL, Manchester, U.K.

## Abstract

Knowledge of the *P-T* location and stoichiometry of the fluid-absent reaction Phl + Qtz = En + Sa + M is required for a better understanding of crustal anatexis and crystallization and the stability of biotite in granitoid magmas. This equilibrium has been experimentally investigated by Bohlen et al. (1983), Montana and Brearley (1989), and Peterson and Newton (1988, 1989). However, there has been consensus neither on the chemographic relationships among the possible phases involved in this equilibrium nor on its precise *P-T* location. We have carried out experiments, at pressures between 100 and 1500 MPa and temperatures between 800 and 920 °C, in order to remove or explain these uncertainties. The following brackets were obtained for the reaction: 100 MPa, 805–815 °C; 150 Mpa, 798–811 °C; 200 MPa, 808–821 °C; 300 MPa, 810–821 °C; 500 MPa, >838 °C; 800 MPa, 860–865 °C; 1000 MPa, 849–876 °C, 1500 MPa, 909–921 °C. In addition, we reversed the equilibrium at 1000 MPa. Our experiments confirm the presence of sanidine as a reaction product over the pressure range investigated.

Because the reaction Sa + Qtz + Fl = M nearly coincides with Phl + Sa + Qtz + Fl = M and En + Sa + Qtz + Fl = M, it can be considered as an excellent analogue of the solidus in the KMASH system. It is possible to calculate the *P-T* location of this solidus as a function of $a_{H_2O}$ using models for the interactions between $H_2O$ and aluminosilicate melts. Using available thermodynamic data, we can also calculate the shift of the subsolidus reaction Phl + Qtz = En + Sa + Fl as a function of decreasing $a_{H_2O}$. The intersections of these curves, at the same $a_{H_2O}$, provide a theoretical location for the fluid-absent melting reaction. This calculated curve has a slope very similar to, and only 10–15 °C above, our experimental curve. This modeling, together with the composition of the phases, allows us to calculate that the fluid-absent reaction will produce up to 50 ± 15 wt% melt in the pressure range 100–1500 MPa.

On the basis of the experimentally determined locations of the solidus reactions (Phl + Qtz + Sa + Fl = M and En + Sa + Qtz + Fl = M) and the subsolidus equilibrium (Phl + Qtz = En + Sa + Fl), Grant (1986) concluded that there should be a thermal divide on the liquidus below 500 MPa. Our experiments and modeling of the solubility of $H_2O$ in the melts suggest that a thermal divide may well exist but that it must be restricted to a very narrow domain between 65 and 100 MPa, at about 810 °C. Additional components such as Ti and F should have the effect of significantly extending such a thermal barrier.

## Introduction

Around 20 years ago, attention was drawn to the importance of fluid-absent conditions in magmatic and metamorphic processes (Yoder and Kushiro, 1969; Robertson and Wyllie, 1971; Eggler, 1973; Fyfe, 1973). In such settings, melting at geologically attainable temperatures most commonly depends upon the availability of $H_2O$ from crystalline hydrates such as muscovite, biotite, and hornblende. The reaction biotite + quartz = orthopyroxene + potassium feldspar + melt has been used to model fluid-absent melting in common crustal rock types, such as quartzofeldspathic metagraywackes (Grant, 1973; Clemens and Wall, 1981). The simplest end-member equivalent of this reaction is phlogopite + quartz = enstatite + sanidine + melt in the KMASH system (Wones, 1967; Luth, 1967). Quantitative knowledge of the pressure and temperature location of this reaction is therefore required for a better understanding of crustal anatexis.

This reaction has been experimentally investigated by Bohlen et al. (1983), Montana and Brearley (1989), and Peterson and Newton (1988, 1989). However, there is consensus neither on the chemographic relationships among the possible phases involved in this equilibrium, nor on the pressure-temperature location of the reaction, in particular at 1000 MPa ($T$ = 890–900 °C, Bohlen et al., 1983; 815–850 °C, Peterson and Newton, 1988; 835–850 °C, Montana and Brearley, 1989). One purpose of

0003–004X/92/1112–1206$02.00

this study is to remove or propose explanations for these uncertainties.

On the basis of the experimentally determined locations of the solidus curves Phl + Qtz + Sa + Fl = M and Qtz + Sa + En + Fl = M, and the subsolidus equilibrium Phl + Qtz = Sa + En + Fl, Grant (1986) concluded that there should be a thermal divide on the liquidus below 500 MPa. Below this point, there would be two fluid-absent reactions: Phl + Sa + Qtz = En + M and Phl + Qtz = En + M (Fig. 1c). So few experiments have been performed at low pressure on the fluid-absent melting of phlogopite + quartz that it is impossible to verify the existence and location of any such singular points and thermal divide.

It has been shown earlier (Clemens and Vielzeuf, 1987) that the simple melting reactions in the Qtz-Ab-Sa-$H_2O$ system and subsystems are good models for melting reactions in more complex systems. This is valid for systems involving MgO as an additional component (e.g., Phl + Qtz + Sa + Fl = M). In the simple systems, it is possible to calculate the *P-T* location of the solidus as a function of $a_{H_2O}$ (Burnham, 1979; Burnham and Nekvasil, 1986; Nekvasil and Burnham, 1987; Nekvasil, 1988). Using available thermodynamic data, it is also possible to calculate the shift of the subsolidus reaction Phl + Qtz = En + Sa + Fl as a function of decreasing $a_{H_2O}$. The intersections of these curves provide a theoretical location for the fluid-absent reaction which, if correct, must tally with the experimentally determined location.

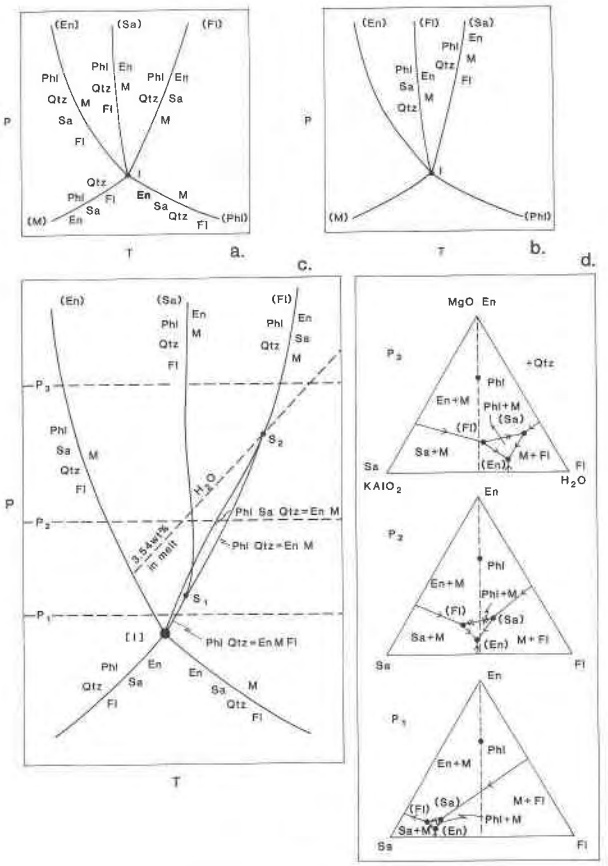


Fig. 1. Topological relationships around invariant point (I) in the system $KAlO_2$-MgO-$SiO_2$-$H_2O$. (**a**) The $H_2O$ content in the melt at the invariant point is greater than about 3.5 wt%, and phlogopite + quartz breakdown cannot provide enough $H_2O$ to saturate the melt (Luth, 1967). (**b**) The $H_2O$ content of the melt at the invariant point is lower than about 3.5 wt%, and phlogopite + quartz is able to saturate the melt (Grant, 1986). Experiments and modeling indicate that the situation in **b** is correct in the immediate vicinity of the invariant point. With increasing pressure, the $H_2O$ content of the melt increases, and the relative arrangement of reactions (En), (Sa), and (Fl) must change from case **b** to case **a**, thus creating singular points. (**c**) Illustration of singular points resulting from a change in reaction topologies from those in **b** to those in **a**. (**d**) Schematic liquidus diagrams are shown for three pressures given in **c**. The MgO contents of the liquids are greatly exaggerated for clarity. In **c**, no thermal barrier can exist above the dashed line, which corresponds to a melt $H_2O$ content of 3.54 wt% (see text). All these figures are modified after Grant (1986); see also Eggler (1973) and Eggler and Holloway (1977). Abbreviations for phases are: Phl = phlogopite, Qtz = quartz, Sa = high sanidine, En = orthoenstatite, Fl = supercritical aqueous fluid, and M = hydrous silicate melt. Other abbreviations used in the text include Ab = $NaAlSi_3O_8$, Or = $KAlSi_3O_8$.

## Previous experiments

In this section we recapitulate the experimental results obtained by previous workers. Later, we will critically evaluate all experimental work and present what we believe to be the most consistent interpretation.

Bohlen et al. (1983) reported 16 experiments on the fluid-absent melting of phlogopite + quartz. For the starting materials, Brazilian quartz was finely ground, leached in $HNO_3$, and fired at 800 °C for 48 h. Phlogopite was prepared from $K_2CO_3$, MgO, $Al_2O_3$, and $SiO_2$, reacted hydrothermally. Actual starting materials were mixtures of phlogopite and quartz (1:5 mole ratio, ~1.3:1 by weight). The loaded, but open, capsules were dried in a vacuum oven at 150 °C for 30 min. After sealing, the capsules were placed into larger Pt capsules with sintered hematite, to maintain low $f_{H_2}$ in the inner capsule. The experimental apparatus was a 2.54-cm piston cylinder used with NaCl pressure cells and graphite tube furnaces. Calibration methods are detailed in Bohlen and Boettcher (1982), and we estimate *P* and *T* uncertainties to have been about ±20 MPa and ±5 °C. Most experiments had rather short durations (usually 24 h).

Bohlen et al. proposed the following five brackets, as indicated in Figure 2: 500 MPa (850–860 °C), 750 MPa (870–880 °C), 1000 MPa (890–900 °C), 1500 MPa (910–920 °C), 2000 MPa (910–920 °C).

In these experiments, the solidus was determined by the abrupt appearance of large proportions of finely intergrown enstatite, sanidine, and glass. The authors observed that the reaction of phlogopite + quartz to enstatite + sanidine + melt is rapid, with 50–70% of the reaction occurring within 24 h, and that the reverse reaction is extremely sluggish. Another point of interest is

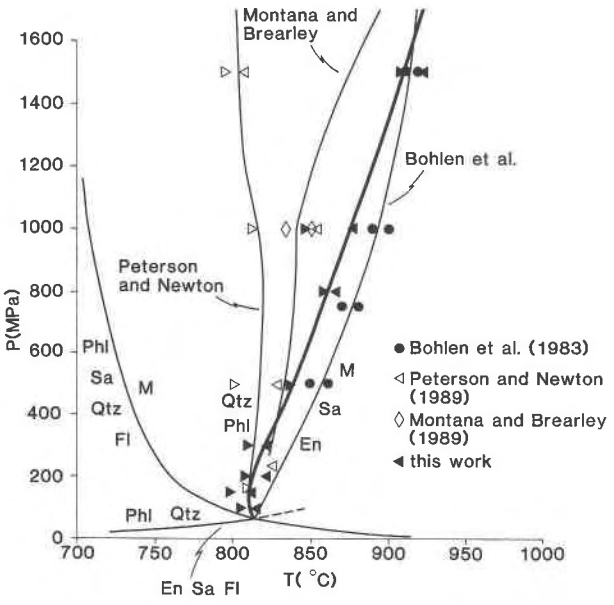


Fig. 2. Summary of experimental brackets on the fluid-absent reaction Phl + Qtz = En (+ Sa) + M. The *P-T* locations of reactions Phl + Qtz = En + Sa + Fl (Wood, 1976; Wones and Dodge, 1977; Peterson and Newton, 1989) and Phl + Sa + Qtz + Fl = M, nearly coincident with Sa + Qtz + Fl = M (Luth, 1967; Bohlen et al., 1983; Peterson and Newton, 1989), are shown.

that Bohlen et al. reported the systematic appearance of sanidine in their products, though the identification method was not stated.

Some more recent data on phlogopite + quartz melting reactions are those of Peterson and Newton (1988, 1989). In their experiments, phlogopite was synthesized from mixtures of $K_2CO_3$ or $KNO_3$, $Al_2O_3$ or $Al(OH)_3$, and MgO and fused silica. Mixtures were reacted, in cold-seal vessels, with 10–20 wt% distilled $H_2O$, at 100 MPa and 800 °C for 10 d. X-ray characterization indicated that micas were slightly nonstoichiometric phlogopites [$V$ ranging from = 495.4 (± 0.2) Å$^3$ to 497.0 (± 0.1) Å$^3$], corresponding to a maximum possible total excess Al content (octahedral and tetrahedral) of approximately 0.4 cations per 12 O atoms (Peterson and Newton, 1989). Starting batches of phlogopite and quartz (2:3 or 3:2 by weight) were ground in an agate mortar, under distilled $H_2O$, to a fine-grained homogeneous mixture. Samples were dried at 80°C for 1 h, then for 1–2 h at 110 °C, immediately before sealing of the Au or Pt capsules. Above 600 MPa, experiments were conducted in a 1.91-cm (and more rarely in a 2.54-cm) piston-cylinder apparatus, with NaCl cells as the pressure media. Sample capsules were embedded either in NaCl or Ca-Na soft glass. Experiments in the range 30–600 MPa were conducted in an internally heated Ar pressure vessel. The duration of these experiments varied from 2 to 60 d. Aside from single-stage experiments, there were also some two-stage ones. In these, $T$ was first raised to 950 °C for ~80 h and then held for ~200 h at a lower temperature.

Peterson and Newton (1989) located the melting of phlogopite + quartz at ~810 °C at 160 MPa, <825°C at 240 MPa, 800–830 °C at 500 MPa, 815–850 °C at 1000 MPa, 795–805 °C at 1500 MPa, and 800–810 °C at 1800 MPa (Fig. 2). The criterion for melting was the presence of enstatite and glass in the products. They also investigated the effects of $H_2$ by isolating their samples from $H_2$ flux during the experiments. This was done by placing hematite or glass around the capsules. They concluded that the temperature of the fluid-absent reaction (Fl) under $f_{O_2}$ conditions equivalent to the hematite-magnetite buffer was consistent with the results of unbuffered experiments.

In their two-stage experiments at 1000 MPa Peterson and Newton (1989) found a temperature interval (815–850 °C) over which phlogopite, quartz, orthopyroxene, and liquid coexisted. Neither original nor regrown phlogopite was detected in the products of experiments at $T$ above 850 °C. The reversal bracket reported in their Figure 2 indicates that fluid-absent melting occurs between 790 and 850 °C, the lower limit being the maximum temperature for which the starting mixture of phlogopite + quartz appeared unreacted. Within the interval 815–850 °C, they reported that the mica and coexisting pyroxene both become less aluminous as $T$ increases. Their analytical data suggest that the maximum extents of aluminous end-member substitutions are 20 mol% in the mica and 7 mol% in the orthopyroxene.

Sanidine was not detected in any of the experimental products, though the samples were examined using petrographic, scanning electron microscope, electron microprobe, and X-ray diffraction techniques. This led these authors to conclude that the fluid-absent breakdown of phlogopite + quartz corresponds to a thermal divide (Phl + Qtz = En + M), in agreement with Grant's (1986) topology. According to them, this thermal divide would extend to pressures greater than 1800 MPa. Thus, the singular point corresponding to the high-pressure end of the thermal divide would be located at an even greater pressure.

Noting the discrepancy between the results of Bohlen et al. (1983) and Peterson and Newton (1988), Montana and Brearley (1989) decided to investigate the fluid-absent melting of phlogopite + quartz at 1000 MPa, in a 2.54-cm piston-cylinder apparatus. The experimental procedures were similar to those described by Bohlen et al., except that the interior of the furnace was made of BN and MgO. Type-S Pt-Rh thermocouples were used and a hematite-magnetite buffer seems to have been employed in a double-capsule configuration. Durations were varied between 200 and 624 h.

These authors reported nine experiments at 1000 MPa and temperatures between 825 and 950 °C and located the reaction between 835 and 850 °C (Fig. 2). They attributed the disagreement with the bracket proposed by Bohlen et al. (1983) to the demonstrably sluggish kinetics

of the reaction, coupled with insufficient durations in the Bohlen et al. experiments. Montana and Brearley (1989) considered the reversed experiments reported by Peterson and Newton (1989) to be inadequate to establish the beginning of melting at 815 °C. The coexistence of phlogopite and liquid in the two-stage experiments of Peterson and Newton between 815 and 835 °C is explained as the metastable persistence of melt after the temperature was dropped from 950 °C to the final value.

Montana and Brearley (1989) never identified sanidine with any certainty among their products. They concur with Peterson and Newton (1988) that potassium feldspar is "a minor or an unnecessary phase in this reaction" and postulate the existence of a thermal barrier up to about 300 MPa.

## The fluid-absent melting of phlogopite + quartz revisited

### Experimental techniques

**Apparatus.** The lower pressure experiments ($P \leq 300$ MPa) were conducted in cold-seal vessels with vertically mounted furnaces (the hot spot on top of the vessel) and used $N_2$ (with trace $H_2O$) as the pressure medium. Temperatures were measured with external, type-S thermocouples and are believed accurate to ±5 °C. Thermal gradients were measured with an internal type-K thermocouple at 1 atm and 800 °C and amounted to <1 °C over 2 cm at the sample locations in the vessels. Ceramic filler rods were used to minimize the free fluid volume and, given the width of the furnace hot spots, we anticipate almost no convection and gradients ≪1 °C across the tiny capsules. Pressure was monitored using a solid-state transducer accurate to ±0.6 MPa. Week-long experiments at 100 MPa and 800 °C, with Pt capsules containing various metal oxides and $H_2O$, showed that the intrinsic $f_{O_2}/f_{H_2}$ of the system is close to $Fe_3O_4 + Fe_2O_3 + H_2O$ or $Cu + Cu_2O + H_2O$.

All of the experiments reported in this study were carried out at Clermont-Ferrand except one 500 MPa experiment, which was performed in a small-volume, internally heated pressure vessel in the Department of Chemistry at Arizona State University. The vessel used there was held horizontally, and the pressure medium was Ar. The samples were heated by a single-zone, wire-wound resistance furnace. Pressure was measured by a manganin resistance cell, which was calibrated against a Heise gauge. Temperatures were monitored by type-K thermocouples and are accurate to ±2 °C.

Experiments conducted in the gas apparatus at 800 and 1000 MPa were carried out in a 1500 MPa large-volume, internally heated vessel. The vessel was positioned horizontally, with a pressure medium of $N_2$, and the samples were heated by a single-zone, Pt furnace. Pressure was measured by a manganin cell calibrated at the International Bureau des Poids et Mesures in Paris. A recent comparison of the pressure measured by this cell and a factory-calibrated Heise gauge (1–7000 bars) indicated a pressure difference of less than 5 MPa at 450 MPa. Temperatures were monitored by type-B thermocouples located immediately adjacent to each of the capsules and are accurate to ±10 °C.

Most higher pressure experiments were carried out in a 1.27 or 1.91-cm piston-cylinder apparatus that was not end loaded (Patera and Holloway, 1982).

In the piston-cylinder experiments, pressure cells 1.27 cm in diameter were all NaCl or NaCl-Pyrex or, more rarely, talc-pyrex, with graphite furnace tubes. The insides of the graphite furnaces were filled with rods of NaCl or borosilicate glass and cylinders of crushable magnesia. Temperatures were measured with Pt-Rh (type-S) or $WRe_5$-$WRe_{26}$ (type-C) thermocouples, calibrated against the 1000-MPa melting point of Au (1120 °C, Akella and Kennedy, 1971). Thermal gradients of ~2 °C across the samples 0.6 mm thick are estimated from the measurements of Esperança and Holloway (1986) and Jakobsson and Holloway (1986) on this type of sample assembly. Reported temperatures are considered accurate to ±5 °C. Temperature was controlled to ±1 °C and pressure generally to ±10 MPa.

In additional experiments using the piston cylinder, the pressure assemblies, 1.91 cm in diameter, were nearly the same as those described by Perkins et al. (1981). They comprised an outer NaCl bushing surrounding a glass sleeve, which in turn surrounded the graphite furnace. Inside the furnace, an additional glass sleeve, cored by crushable magnesia, served as the pressure medium. At the core, the small flat Pt capsule was surrounded by crushed borosilicate glass. A type-C thermocouple, protected by an alumina ceramic, passed through a small hole in the magnesia. The thermocouple tip was protected by a small amount of BN powder and separated (by <1 mm) from the Pt capsule by a thin magnesia wafer. Independent temperature calibration experiments suggest that the difference between the temperature at the thermocouple tip and the capsule is less than 5 °C. Perkins et al. (1981) found that a pressure correction of −5 to −11% should be applied to the salt-glass assembly. In order to check this, the fayalite + anorthite = grossular + almandine reaction was reversed in an internally heated gas apparatus at 700 MPa (Perkins and Vielzeuf, 1992) and the results compared with those from the piston cylinder. This study suggests that a pressure correction of between −4 and −8% should be applied to nominal pressures. Another set of pressure calibration experiments was conducted by D. Laporte at 500 and 1500 MPa, using the melting point of NaCl and the falling ball technique (Bohlen, 1984; Cemic et al., 1990). These experiments indicate that no pressure correction need be applied at 1500 MPa, whereas a positive correction of ~7% should be applied at 500 MPa. The apparent discrepancy with the other pressure calibration is not understood, and no pressure correction was applied.

In piston-cylinder experiments, a cold pressure of 150 MPa was initially applied to the assembly. The temperature was then raised to approximately 510 °C, at which

point the pressure ceased to increase and began to decrease. At that stage, the desired final pressure could be applied without shattering the cell.

**Experimental procedures.** For experiments at $P \leq 200$ MPa, thin-walled Pt capsules (3 mm od × 10 mm × 0.1 or 0.15 mm) were welded shut on one end and loaded with about 0.02 g of starting material. The capsules were squashed flat and lightly crimped, dried at 130 °C for at least 2 h, and then promptly sealed with a C arc welder.

In the experiments at higher $P$, the same initial procedure was followed, but then the capsules were squashed flat and folded into packets with approximate dimensions of 3.5 × 5 × 0.6 mm. These packets lay flat in the pressure cells so that the samples would experience the minimum possible thermal gradients.

All experiments were simultaneously brought to final $P$-$T$ conditions, and we used the hot piston-in technique for the solid-medium experiments. Experimental conditions were monitored and recorded several times per day over the course of an experiment. Reported temperatures are the averages of the minimum and maximum recorded, and quoted uncertainties represent the total ranges of temperature variation during the experiments. A similar procedure was followed for the pressure measurements. To avoid vesiculation of volatile-bearing glasses, all experiments were quenched isobarically. Quench rates were of the order of 100 °C/s in the piston cylinders, 3 °C/s in the cold-seal vessels (cooled by air jet) and 1 °C/s in the internally heated vessels.

After the experiment, capsule integrity was checked by microscopic examination and, when possible, by comparing post- with pre-experiment masses.

**Starting materials.** Phlogopite was synthesized from $KAlSi_3O_8$ gel plus MgO and excess $H_2O$. A small aliquot of the gel-oxide mix was fused to a glass on an Ir strip heater (Nicholls, 1974). Electron probe analysis of this glass showed that it has the correct stoichiometric composition. Phlogopite synthesis conditions were 200 MPa, 800 °C, and 122 h. Optical and X-ray examination of the product revealed no impurities. X-ray powder diffractometry yielded the following cell constants: $a = 5.317(6)$ Å, $b = 9.215(7)$ Å, $c = 10.322(8)$ Å, $\beta = 100°1'(4')$, and $V = 498.0(5)$ Å$^3$, where the figures in parentheses are $2\sigma$ uncertainties. The $d_{060}$ value is 1.5364 Å, implying the absence of both octahedral site vacancies (Robert, 1976) and Fe contamination (Wones, 1963). Within uncertainties, our phlogopite is identical to that of Yoder and Eugster (1954) in its cell parameters. Compared to that of Hewitt and Wones (1975), our phlogopite is, again, almost identical; it has slightly larger $c$ and $\beta$, but the cell volume is the same within error. No analyses were made because the crystals were much too small to probe.

All quartz used in our experiments was finely ground ($<10$ μm), acid-washed, Brazilian, optical-grade rock crystal.

The tetraethyl orthosilicate (TEOS) used as a source of $SiO_2$ in the sanidine gel was standardized, in triplicate, to give 28.686 ± 0.034 wt% $SiO_2$. The $H_2O$ used was distilled, deionized $H_2O$ in all cases.

The starting mixture was made by grinding the pure, synthetic phlogopite and quartz together, in a mechanical agate ball mill, under acetone, for 20 min. The mixture contained phlogopite and quartz in equal mass proportions, so that all products were saturated in excess quartz. The mix was dried at 110 °C and stored in a vacuum desiccator over silica gel.

**Observation and analysis of products.** The combined use of various observational and analytical techniques proved essential for the interpretation of the products. The contents of each capsule were split into several portions. Part was ground and used to make an optical grain mount. Microscopic examination of these grain mounts was an important method of phase identification. X-ray powder diffractometry and SEM observations were used for (1) the detection of sanidine, since light-optical identification was difficult, (2) the detection of enstatite at low pressure, and (3) gauging the extent of the reaction by comparing the relative intensities of the diagnostic phlogopite, quartz, and enstatite peaks.

A CGR diffractometer was used with Cu$K\alpha$ radiation and calibrated between each sample, using Au and quartz standards.

Some electron probe analyses were carried out on a Cameca Camebax Micro fitted with a Link energy-dispersive system. For the analyses, three crystal spectrometers were used, the accelerating potential was 15 kV, and the probe current was about 10 nA with a 2-μm beam diameter. Specimens were C coated and counting times were 10 s per series of three elements. Standards were natural minerals, and ZAF correction procedures were applied.

The electron beam instrument at Manchester (used for examination of products, photomicrography, and some analyses) is a JEOL JSM 6400, fitted with a Link EXL energy-dispersive analytical system and an Oxford Instruments freezing stage. We used ZAF4 software for the data processing. Probe analyses of quenched melts (glasses) were carried out using an accelerating potential of 15 kV and a probe current of 1.50 nA. The sample temperature was held at −193.5 °C and the counting time was 40 s. In order to obtain a good count rate with such a weak beam, a large-diameter Be window was fitted to the detector. These measures effectively eliminated any diffusion-related counting losses on light elements (e.g., Mg and K). Tests using a similar method on a sample of $NaAlSi_3O_8$ glass containing 9 wt% $H_2O$ yielded analyses that correspond closely to those obtained on the anhydrous equivalent, which was prepared by 1-atm fusion of the same gel starting material. Figure 3 shows SEM photomicrographs of some products.

**Identification and description of phases in the products.** In all experimental products, most phlogopite forms very fine-grained masses in which individual crystals are commonly difficult to distinguish. However, some products

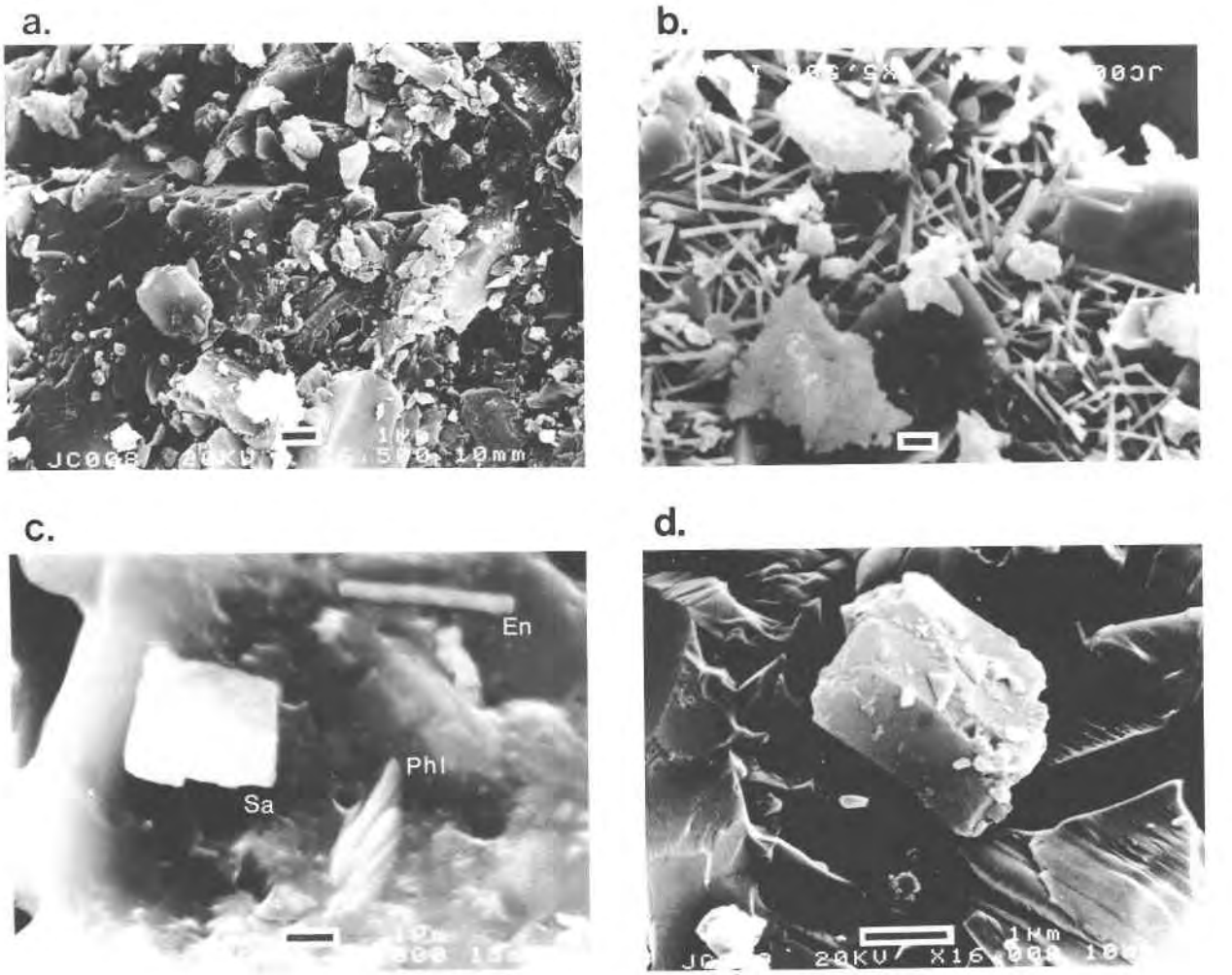


Fig. 3. SEM secondary electron photomicrographs of some experimental products. The scale bars represent 1 $\mu$m in all cases. (**a**) Unreacted phlogopite + quartz from experiment K-44 (800 MPa, 850 °C, 312 h). (**b**) Matted enstatite needles and glass fragments produced in experiment K-17 (200 MPa, 820 °C, 280 h), in which the fluid-absent melting reaction has gone almost to completion. (**c**) Relict phlogopite + new enstatite and sanidine crystals in a matrix of quench glass from low-pressure experiment K-30 (150 MPa, 838 °C, 241 h). (**d**) Sanidine crystal and glass formed in high-pressure experiment K-34 (1500 MPa, 920 °C, 130 h).

contain a few crystals that attain a respectable size ($\leq$10 $\mu$m). These larger grains are colorless and have medium relief that varies with crystal orientation, high birefringence, and straight extinction. The 001 reflection, at about 10.10 Å, was used to identify this phase on XRD traces.

Quartz grains in supersolidus products are commonly larger ($\leq$25 $\mu$m) than in the starting material. The larger grains have a rounded, subhedral, $\beta$ habit.

The forms of enstatite crystals vary dramatically. At 1000 and 1500 MPa, enstatite usually forms stubby prisms with length/width ratios averaging <3. All of these have straight extinction, and none attains great size. One of the great surprises in our experiments was the form of the enstatite in experiments at low $P$ ($\leq$300 MPa). Here, the enstatite is optically indistinguishable from the very fine-grained, equigranular phlogopite aggregates that exist in the subsolidus region. The products of these low-$P$ experiments are, in fact, so fine-grained that we were able to identify the phases present only with X-ray diffractometry or SEM examination. Figure 3b shows the extremely small and fine enstatite needles formed in one of these low-pressure experiments. The 610 reflection, at about 2.87 Å, was used to positively identify this phase using XRD.

Sanidine was not identified optically, but its presence was detected through characteristic X-ray reflections (corresponding to $\bar{2}01$, 130, $\bar{2}02$, 002, 131, and 060 planes) and its crystal form and composition, as seen in the SEM and microprobe. This potassium feldspar is always in the high structural state, as confirmed by the X-ray methods of Wright (1968), and forms rhombic-looking prisms <5 $\mu$m across (see Fig. 3c, 3d). The 040 reflection, at 3.23 Å,

**TABLE 1** Experimental results

| Expt. no. | Machine and assembly | Thermocouple | $P$ (MPa) | $T$ (°C) | Duration (h) | Assemblage | Remarks |
|---|---|---|---|---|---|---|---|
| K-64 | EHPV | S | 100 ± 0.5 | 806 ± 1 | 240 | Phl + Qtz | unconsolidated powder |
| K-65 | EHPV | S | 100 ± 0.5 | 814 ± 1 | 351 | (Phl +) Qtz + En (+ Sa) + Gl | hard and brittle, strong decrease of Phl and Qtz, sanidine present |
| K-32 | EHPV | S | 151.3 ± 0.7 | 800 ± 2 | 263 | Phl + Qtz | soft and crumbly |
| K-33 | EHPV | S | 151.3 ± 0.7 | 810 ± 1 | 263 | (Phl +) Qtz + En + Gl | hard and brittle, pseudomorphs of En after Phl |
| K-28 | EHPV | S | 150.2 ± 1.1 | 819 ± 2 | 265 | (Phl +) Qtz + En + Gl | |
| K-29 | EHPV | S | 150.2 ± 1.1 | 830 ± 1 | 235 | Qtz + En + Gl | hard and brittle |
| K-30 | EHPV | S | 150.2 ± 1.1 | 838 ± 4 | 241 | ((Phl)) + Qtz + En ( + Sa) + Gl | hard and brittle, sanidine present |
| K-12 | EHPV | S | 200.2 ± 0.9 | 800 ± 1 | 263 | Phl + Qtz | |
| K-13 | EHPV | S | 200.2 ± 0.9 | 812 ± 4 | 242 | Phl + Qtz | |
| K-17 | EHPV | S | 198.6 ± 1.1 | 820 ± 1 | 280 | (Phl +) Qtz + En + Gl | hard |
| K-18 | EHPV | S | 199.3 ± 0.8 | 830 ± 1 | 140 | (Phl +) Qtz + En + Gl | hard |
| K-35 | EHPV | S | 299.7 ± 1.2 | 811 ± 1 | 238 | Phl + Qtz | |
| K-36 | EHPV | S | 299.7 ± 1.2 | 820 ± 2 | 238 | (Phl +) Qtz + En + Gl | hard and brittle |
| K-62 | EHPV | S | 300 ± 5 | 820 ± 1 | 352 | (Phl +) Qtz + En + Gl | |
| K-63 | EHPV | S | 300 ± 2 | 820 ± 1 | 470 | Phl + Qtz (+ En) + Gl | |
| K-43 | IHPV | K | 503.3 | 841 ± 3 | 168 | Phl + Qtz | |
| K-44 | IHPV | B | 800 ± 7.5 | 850 ± 7 | 312 | Phl + Qtz | unconsolidated powder |
| K-48 | IHPV | B | 800 ± 2.5 | 845 ± 5 | 306 | Phl + Qtz | |
| K-47 | IHPV | B | 800 ± 2.5 | 865 ± 5 | 306 | Phl + Qtz | |
| K-46 | IHPV | B | 800 ± 2.5 | 875 ± 5 | 306 | Phl + Qtz + En (+ Gl) | hard and brittle |
| K-51 | IHPV | B | 800 ± 5 | 863 ± 2 | 358 | ((Phl)) + Qtz + En + Gl | |
| K-7 | PC ½ in., all salt | C | 999 ± 23 | 830 ± 1 | 215 | Phl + Qtz | |
| K-15 | PC ½ in., all salt | C | 1004 ± 21 | 840 ± 1 | 193 | Phl + Qtz | |
| K-25 | PC ½ in., all salt | C | 1011 ± 19 | 850 ± 1 | 208 | Phl + Qtz | |
| K-6 | PC ½ in., all salt | C | 1005 ± 14 | 860 ± 1 | 156 | Qtz + En + Sa + Gl | sanidine present |
| K-4 | PC ½ in., all salt | C | 1008 ± 17 | 880 ± 1 | 113 | Qtz + En + Gl | |
| K-50 | PC ½ in., all salt | C | 996 ± 23 | 880 ± 1 | 18 | Phl + Qtz | short duration equivalent of K-4 |
| K-38 | PC ½ in., all salt | S | 1012 ± 13 | 860 ± 1 | 168 | Phl + Qtz | |
| K-39 | PC ½ in., all salt | S | 1010 ± 14 | 880 ± 1 | 176 | (Phl +) Qtz + En + Gl? | |
| K-40 | PC ½ in., all salt | S | 993 ± 6 | 900 ± 1 | 32 | Qtz + En + Gl | |
| K-41 | PC ½ in., TP | C | 987 ± 16 | 890 ± 1 | 166 | Qtz + En + Gl | |
| K-49 | PC ½ in., TP | C | 1002 ± 16 | 880 ± 1 | 168 | Phl + Qtz (+ En) + Gl | |
| K-52 | PC ½ in., TP | C | 998 ± 23 | 870 ± 1 | 218 | (Phl? +) Qtz + En + Gl | |
| K-53 | IHPV | B | 1002 ± 2 | 872 ± 4 | 284 | Phl + Qtz (+ En) + Gl | |
| K-54 | IHPV | B | 1002 ± 2 | 888 ± 1 | 284 | Phl + Qtz (+ En) (+ Gl?) | |
| K-55 | PC ¾ in., SP | C | 995 ± 6 | 870 ± 1 | 168 | Phl + Qtz (+ En) + Gl | |
| K-56 | PC ¾ in., SP | C | 1001 ± 9 | 890 ± 1 | 156 | Phl + Qtz (+ En) + Sa? + Gl | probable sanidine detected by XRD |
| K-57 | PC ¾ in., SP | C | 998 ± 7 | 900 ± 1 | 168 | (Phl +) Qtz + En + Gl | |
| K-58 | PC ¾ in., SP | C | 1003 ± 7 | 910 ± 1 | 214 | ((Phl)) + Qtz + En + Sa + Gl | sanidine present |
| K-59 | PC ¾ in., SP | C | 1002 ± 9 | 920 ± 1 | 183 | ((Phl)) + Qtz + En + Gl | |
| K-60 | PC ¾ in., SP | C | 999 ± 7 | 910 ± 1 | 168 | ((Phl)) + Qtz + En + Sa + Gl | pseudoreversal, large crystals of En |
| | | | | 875 ± 1 | 167 | | sanidine present |
| K-61 | PC ¾ in., SP | C | 995 ± 7 | 910 ± 1 | 184 | Phl + Qtz ((+ En)) + Gl | pseudoreversal, |
| | | | | 850 ± 1 | 159 | | regrowth of Phl |
| K-26 | PC ½ in., all salt | C | 1506 ± 26 | 870 ± 1 | 192 | Phl + Qtz | |
| K-27 | PC ½ in., all salt | C | 1502 ± 37 | 890 ± 1 | 160 | Phl + Qtz | |
| K-31 | PC ½ in., all salt | C | 1501 ± 25 | 910 ± 1 | 165 | Phl + Qtz | |
| K-34 | PC ½ in., all salt | C | 1491 ± 36 | 920 ± 1 | 130 | (Phl +) Qtz + En + Sa + Gl | sanidine present |

*Note:* EHPV = externally heated pressure vessel, IHPV = internally heated pressure vessel, PC = piston cylinder, TP = talc-Pyrex, SP = salt-Pyrex; ( ) = minor quantity of phase, (( )) = trace.

was used to positively identify this phase on the diffractograms.

In experiments at $P \geq 500$ MPa, colorless, isotropic glass formed easily recognizable patches, interstitial to enstatite crystals. At lower pressures, glass was not readily identifiable by optical means. Its presence was inferred from the brittleness and hardness of the products when they were being crushed in an agate mortar. In some low-$P$ experiments with small extents of reaction, glass was not identified at all; its presence was inferred from the oc-

currence of traces of more easily identifiable enstatite needles. This difficulty results from the sluggishness of phlogopite breakdown at $P < 500$ MPa and $T < 800$ °C.

## Results

About 50 experiments were performed on the fluid-absent melting of phlogopite + quartz at pressures of 100, 150, 200, 300, 500, 800, 1000, and 1500 MPa. In order to understand the behavior of the system, various techniques, sample arrangements, thermocouples, and durations were used. This was done to demonstrate consistency in the results, despite changes in methodology that involve different error margins on variables such as $P$ and $T$. These experiments are reported in Tables 1 and 2.

**Experimental brackets.** Six series of experiments, using variable configurations, were performed at 1000 MPa. The first series was made in a 1.27-cm piston cylinder with type-C thermocouples, using all-salt assemblies. No enstatite grew at $T \leq 850$ °C. The bracket we obtained is 849–861 °C (experiments K-25, K-6). Note that, at 860 °C, sanidine was detected by X-ray and confirmed under the electron microprobe. In the same experiment, both the sanidine and the glass had significant Na contents, though no Cl was detected. This indicates possible contamination by Na diffusion through the Pt capsules. A short-duration experiment (K-50, 18 h) at 880 °C showed no growth of enstatite, confirming sluggish reaction kinetics, in agreement with the observations of Montana and Brearley (1989) and Peterson and Newton (1989). A second series was performed with type-S thermocouples and similar assemblies. This provided a bracket between 859 and 879 °C (experiments K-38, K-39). The third series used 1.27-cm talc-Pyrex-magnesia assemblies with type-C thermocouples. This series indicates that the reaction begins at $T < 871$ °C. Additional experiments were performed in an internally heated pressure vessel. At 888 °C, reaction is extensive. Rare crystals of enstatite were observed at $T = 872 \pm 4$ °C, indicating proximity to the solidus. The fifth series was performed in a 1.91-cm piston cylinder using NaCl-glass assemblies and type-C thermocouples. The study of the products indicated clearly that X-ray examination is insufficiently sensitive to determine the beginning of melting. The characteristic peak of enstatite, at 31° $2\theta$, did not appear at $T < 900$ °C, though enstatite was optically identified at lower $T$. Peterson and Newton (1989) also observed that the 610 peak of enstatite was suppressed and that the 420 peak at 28.2° $2\theta$ proved more reliable (J. W. Peterson, written communication, 1992). These experiments indicate that the fluid-absent melting of phlogopite + quartz begins at $T < 871$ °C.

In order to constrain the location of the reaction more accurately, we performed pseudoreversals similar to those described by Peterson and Newton (1989). A definition of a reversal is that the equilibrium can be approached from both sides. This means that the product phases grow from the reactants in one direction, and the reactants grow from the products in the other. There is no requirement for complete conversion in either direction. If we demonstrate that we grew En + Sa + M from Phl + Qtz and that we see an increase in Phl + Qtz plus a decrease in En + Sa + M when such products are held at a lower $T$, we have demonstrated reversibility. This will never be proof of equilibrium, however. The "pseudo" character of our reversal arises from the fact that we did not actually open the capsule and prove that the particular product had En + Sa + M in it before we lowered the $T$, though it is very likely, considering the number of experiments we performed at high $T$ and the reproducibility of the results. Pseudoreversal is our term for these two-stage experiments, and we consider that they represent the best way to change only one parameter without affecting the others.

**TABLE 2.** Summary of brackets for the Phl + Qtz = En + Sa + M between 100 and 1500 MPa

| $P$(MPa) | $T$(°C) | Expt. no. |
|---|---|---|
| 100 | 805–815 | K-64, K-65 |
| 150 | 798–811 | K-32, K-33 |
| 200 | 808–821 | K-13, K-17 |
| 300 | 810–821 | K-35, K-63 |
| 500 | >838 | K-43 |
| 800 | 860–865 | K-47, K-51 |
| 1000 | 849–876 | K-60, K-61* |
| 1500 | 909–921 | K-31, K-34 |

* Pseudoreversal experiments.

In our pseudoreversals, the temperature was brought up to 910 °C for 7 or 8 d and then dropped to the desired value. At 875 °C, there was no optical evidence of phlogopite regrowth, though some rare crystals were detected under the SEM. Microprobe work also indicated the presence of sanidine. In the experiment where $T$ was dropped to 850 °C, extensive phlogopite regrowth occurred; enstatite was detected neither optically nor by XRD, though it was found under the SEM. Unless there are kinetic problems preventing the nucleation of the phlogopite, the reaction must be located between 849 and 876 °C (experiments K-60, K-61). In summary, at 1000 MPa, the bracket for the reaction is 849–876 °C and possibly 859–861 °C (if we are optimistic). The full set of brackets between 100 and 1500 MPa is given in Table 2.

Sanidine was detected in various products at different pressures (experiment K-34 at 1500 MPa; experiments K-6, K-58, K-60 at 1000 MPa; experiment K-30 at 150 MPa; and experiment K-65 at 100 MPa), clearly indicating that the melting reaction is Phl + Qtz = En + Sa + M. Consequences for the topology of phase relationships will be discussed later.

All these experimental brackets are shown in Figure 2. They imply a slightly curved reaction boundary for the fluid-absent breakdown of phlogopite + quartz. Taking into account all additional uncertainties and the various experimental techniques and procedures used in this study, we find that the entire length of the reaction approximates

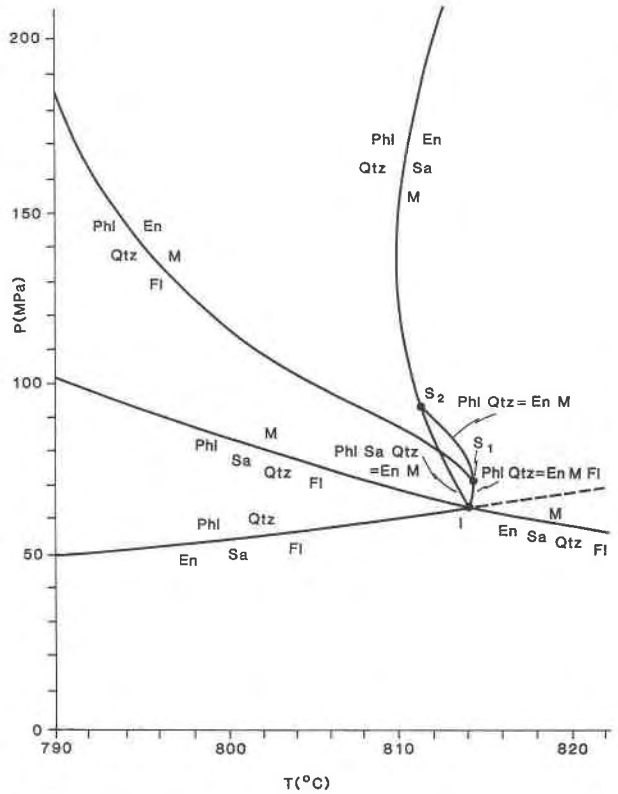


Fig. 4. Enlargement of the relations in the vicinity of the invariant point. Note the highly magnified temperature scale. A decrease in temperature of the invariant point (I) of less than 10 °C would be sufficient to render the slope of the (Fl) reaction positive all the way through.

a straight line [$P$(MPa) = 14.06 $T$(°C) − 11305], provided we accept an error not greater than ±10 °C. However, there is no reason why this reaction should be linear in the $P$-$T$ plane, nor is it necessarily a simple curve. Indeed, the change from a positive to a negative slope, at about 150 MPa (Fig. 4), seems to be rather well constrained and consistent with our preferred location of the invariant point at 815 °C and 65 MPa, based on the available data on the solidus and subsolidus equilibria. However, considering the errors involved in all the experimental data used to locate the invariant point, the slope of the fluid-absent reaction could remain positive all the way through, providing that we select the low-$T$ extreme for the location of the invariant point. A decrease of about 10 °C of the temperature of this invariant point would be sufficient (Fig. 4).

It could be argued that the disappearance of phlogopite should be considered as indicative of the location of the fluid-absent melting reaction. The presence of some enstatite, at lower $T$, would then be viewed as a result of the presence of moisture, which is impossible to remove from the starting material, and thus the result of the incipient reaction Phl + Qtz + $H_2O$ = En + M. However, our experiments, together with the data from Montana and Brearley (1989), clearly show that phlogopite may persist metastably to rather high temperatures. We thus believe that the appearance of enstatite is the best marker of the initiation of the reaction. We attribute the coexistence of phlogopite + quartz + melt + enstatite ± sanidine to kinetic problems.

**TABLE 3.** Compositions of phases analyzed in products of 1000 and 1500 MPa experiments

| | Phl ($n$ = 3)* | Pure Phl |
|---|---|---|
| **Experiment K-61 (1000 MPa, 910–850 °C)** | | |
| $SiO_2$ | 44.77(1.14) | 43.19 |
| $Al_2O_3$ | 12.10(0.41) | 12.22 |
| MgO | 27.24(0.14) | 28.98 |
| $K_2O$ | 11.57(0.14) | 11.29 |
| $H_2O$ | 4.32 | 4.32 |

| | En | Pure En | Sa | Pure Sa | Glass ($n$ = 15) | Starting material** |
|---|---|---|---|---|---|---|
| **Experiment K-60 (1000 MPa, 910–875 °C)** | | | | | | |
| $SiO_2$ | 60.43 | 59.85 | 64.89 | 64.76 | 79.38(0.71) | 71.60 |
| $Al_2O_3$ | 0.09 | 0 | 18.00 | 18.32 | 11.55(0.44) | 6.11 |
| MgO | 39.48 | 40.15 | 0 | 0 | 0.81(1.02) | 14.49 |
| $K_2O$ | 0 | 0 | 17.11 | 16.92 | 8.26(0.26) | 5.64 |
| $H_2O$ | 0 | 0 | 0 | 0 | 0 | 2.16 |

| | En ($n$ = 7) | Sa ($n$ = 3) | Glass ($n$ = 14) |
|---|---|---|---|
| **Experiment K-56 (1001 MPa, 890 °C)** | | | |
| $SiO_2$ | 62.02(0.28) | 66.14(1.27) | 77.32(0.76) |
| $Al_2O_3$ | 0.21(0.33) | 15.26(0.51) | 9.61(0.41) |
| MgO | 37.46(0.41) | 0.73(0.46) | 0.74(0.81) |
| $K_2O$ | 0.31(0.20) | 17.87(0.44) | 12.33(0.46) |
| $H_2O$ | 0 | 0 | 0 |
| **Experiment K-34 (1491 MPa, 920 °C)** | | | |
| | En ($n$ = 3) | Sa ($n$ = 4) | Glass ($n$ = 13) |
| $SiO_2$ | 61.33(0.27) | 64.92(0.91) | 77.33(0.70) |
| $Al_2O_3$ | 0.06(0.09) | 16.77(0.61) | 10.85(0.38) |
| MgO | 38.60(0.18) | 0.50(0.36) | 0.30(0.24) |
| $K_2O$ | 0 | 17.82(0.73) | 11.52(0.34) |
| $H_2O$ | 0 | 0 | 0 |

*Note:* The compositions of pure Phl, En, Sa, and the starting material are given for comparison. All compositions are normalized to 100% anhydrous except those of Phl and the starting material. The abbreviation $n$ = number of individual probe analyses. Figures in parentheses are 1$\sigma$ values. Experiments K-60, K-61 analyzed on the Clermont-Ferrand probe; experiments K-34, K-56 analyzed on the Manchester SEM/probe with freezing stage at −193 °C.

* Normalized to 100% with 4.32% $H_2O$.

** Normalized to 100% with 2.16% $H_2O$.

**Phase compositions.** Compositions of phases, as determined by electron probe, are shown in Table 3. Phlogopite was analyzed in the 1000-MPa pseudoreversal experiment K-61, and enstatite, sanidine, and glass in the 1000-MPa pseudoreversal experiment K-60, the 1000-MPa experiment K-56, and the 1500 MPa experiment K-34. All of the analyzed crystalline phases are close in composition to the pure theoretical phases, indicating that the fluid-absent reaction is a truly univariant reaction. Products of K-60 and K-61 were analyzed at Clermont-Ferrand using standard techniques. The glass analysis in K-60 is corundum-normative (C = 2.61%), indicating some counting losses on $K_2O$. The products of K-34 and K-56 were analyzed at Manchester using the sample-freezing technique described above. The glass analyses, in these cases, are not peraluminous, demonstrating es-

sentially no loss of $K_2O$. The solubility of MgO in these melts, in equilibrium with enstatite, sanidine, and quartz, is less than 1 wt%, averaging 0.63% in the three experiments analyzed.

We performed mass-balance calculations, based on the fact that the bulk starting composition must equal a linear combination of the compositions of the products. For these, we used the compositions of the glass formed in the experiment at 1000 MPa, 890 °C. The mixing program includes an error-propagation routine (Provost, 1989). Enstatite, sanidine, and quartz were considered as pure phases, with 0% error (all errors quoted in this paragraph are given in relative percent). A ±2% error was assumed for all the oxides in the calculated composition of the starting material. The greatest uncertainty concerns the composition of the glass (quenched melt), and the following composition was used: $SiO_2$ = 73.46, $Al_2O_3$ = 9.13, MgO = 0.70, $K_2O$ = 11.71, $H_2O$ = 5.00. The $H_2O$ content was calculated from a solubility model (see below), and an appropriately large uncertainty of ±30% was attributed to its value. A ±2% error was assumed for all the remaining oxides. The following results were obtained: quartz = 21.2 ± 5.8 wt%, enstatite = 35.8 ± 2.7, sanidine = 19.4 ± 7.5, melt = 23.7 ± 12.4. On the supposition that sanidine might disappear soon after the beginning of melting, a similar calculation was performed without this phase, yielding quartz = 8.3 ± 6.2 wt%, enstatite = 35.0 ± 3.4, melt = 56.6 ± 5.4. From these numbers, we can balance the following two reactions: 63.4g Phl + 36.6g Qtz = 45.4g En + 24.6g Sa + 30.0g M and 54.5g Phl + 45.5g Qtz = 38.2g En + 61.8g M. It is clear that the quality of these results depends critically on the composition of the melt, which is difficult to obtain. In particular, the amount of melt is directly related to its $H_2O$ content, which has not been determined directly. However, on the basis of our second mass-balance equation, we agree with Peterson and Newton's (1989) statement that, to a first approximation, the volume percentage of melt in the products is close to that of phlogopite entering the reaction. We draw the reader's attention to the fact that this conclusion cannot be simply extended to most natural rocks, in particular because the effect of plagioclase is not considered.

## Discussion

### Critical comparison with previous work

At $P > 250$ MPa, there are major differences in the location of the fluid-absent melting reaction (Fl), according to various workers (see Fig. 2). Below, we consider interpretations of the results of previous experiments, and how the various discrepancies may be explained.

The data of Bohlen et al. (1983) place (Fl) between 887 and 903 °C at 1000 MPa, which is about 25, 50, and 70 °C above the preferred location for the reaction according to us, Montana and Brearley (1989), and Peterson and Newton (1989), respectively.

Bohlen et al. noted that small amounts of glass appeared in some of their products at temperatures well below their inferred position for reaction (Fl). Our experiments indicate that durations in excess of 100 h are required for significant reaction at 1000 MPa. The Bohlen et al. experiments were only around 24 h long. In agreement with Montana and Brearley (1989) and Peterson and Newton (1989), we suggest that the sluggishness of the reaction explains why Bohlen et al. had to greatly overshoot the equilibrium $T$, in order to get detectable reaction in very short durations. Confirmation of this is seen in comparing the results of our experiments K-49 and K-50. These were both at 1000 MPa and 880 °C, but K-50 (showing no reaction) lasted for only 18 h, whereas K-49 (with a definite reaction) lasted for 168 h. This lack of equilibrium would explain the incomplete decomposition of the phlogopite, the reported detection of trace glass at much lower temperatures, and the inability of Bohlen et al. to obtain a reversal on (Fl). Attempts at reversal probably failed because all of the experiments would have been carried out at temperatures in excess of the true equilibrium value. Note that our results at 1500 MPa agree with the data of Bohlen et al. This suggests that the reaction kinetics improve at higher pressure.

Montana and Brearley (1989) locate the reaction in the interval 835–850 °C, about 30 °C below our preferred location at 1000 MPa (but only 14 °C below the lower value of our bracket). Examination of their table of experimental results indicates that there are two possible brackets for this reaction (835–850 or 860–890 °C). Selecting the bracket at 835–850 °C, as they did, is inconsistent with two of their own experiments (nos. 118 and 126), which showed no enstatite growth at $T \geq 850$ °C. Selecting the second bracket (860–890 °C) would be inconsistent with only one of their experiments (no. 216), which produced enstatite at $T = 850$ °C. Montana and Brearley ascribed the absence of enstatite in experiments 118 and 126 to insufficient duration (~200 h compared to 600 h for no. 216) and disregarded the results. According to our study, such a duration is sufficient to initiate melting: for instance, 140 h at 830 °C and 200 MPa (experiment K-18) were sufficient to promote extensive melting. Thus, we prefer the higher temperature bracket of Montana and Brearley because it agrees with the regrowth of phlogopite at 850 °C in both our and Peterson and Newton's (1989) two-stage experiments. Taking this into consideration, there would be no discrepancy with our results at 1000 MPa. Note that, at 2000 MPa, their bracket is consistent with the Bohlen et al. result.

In order to explain the higher temperatures reported by Bohlen et al. at $P \approx 1000$ MPa, Montana and Brearley suggest that Bohlen et al. traced the metastable extension of the thermal barrier. However, this does not explain the reported systematic presence of sanidine in the products of Bohlen et al., the reaction corresponding to the thermal barrier being both sanidine- and fluid-absent.

The data and interpretations of Peterson and Newton (1989) apparently disagree with all other studies, and this problem becomes more pronounced at higher $P$. At 1500

MPa, the discrepancy with the determinations of Bohlen et al., which are consistent with our own results, is greater than 100 °C. A possible explanation is that the starting material used by Peterson and Newton (1989) may not have been completely moisture free prior to the experiments. In our experience, a fine-grained, powdered starting mixture will commonly contain around 0.3 wt% of adsorbed $H_2O$, most of which can be driven off at 110 °C. As noted earlier, the Peterson and Newton starting material was very finely ground under $H_2O$ and, though subsequently dried at 110 °C, may have picked up a higher than usual quantity of tenaciously adsorbed $H_2O$. If the starting material were not perfectly dry, the first melting would occur at the fluid-present reaction (Sa) (see Fig. 1c, 1d). However, the small amounts of melt and enstatite that would form (≤5 and 2.5 vol%, respectively) might easily be overlooked in the products. Further increases in $T$ would result in the progressive dissolution of phlogopite and quartz, with the formation of additional melt and orthopyroxene. This would continue until the $T$ of the true fluid-absent reaction was reached. At that point (860 ± 10 °C), all remaining phlogopite would be consumed. This behavior would explain the low initial melting $T$, the progressive breakdown of phlogopite mimicking a divariant reaction interval, and the final disappearance of phlogopite coinciding with the $T$ of the true fluid-absent reaction. However, it would not explain the observed changes in mica and pyroxene aluminum contents. Perhaps a more likely possibility is that the excess Al in the starting phlogopite could lower the reaction temperature. Indeed, Peterson and Newton (1989) thought that the 35 °C melting interval at 1000 MPa, between 815 and 850 °C, is a region in which aluminous phlogopite progressively melts and becomes more nearly stoichiometric with increasing temperature. They demonstrated the equilibrium composition of the phlogopite within this field by reproducing the Al content in micas in both high-to low and low-to-high temperature experiments. They also observed that the phlogopite present at 1000 MPa and 850 °C is nearly stoichiometric (1.01–1.05 Al cations per formula unit). With an uncertainty of ±10 °C, there is a possible agreement among these data (850 °C), our data (849–876 °C), and the Montana and Brearley (1989) data (835–850 °C) for the 1000 MPa fluid-absent melting of stoichiometric phlogopite + quartz.

This second interpretation solves the problem of the apparent disagreement between the single-stage and two-stage experiments reported by Peterson and Newton (1989) at 1000 MPa. The single-stage experiments indicate the beginning of melting between 800 and 815 °C, whereas, in their two-stage experiments, these authors detected regrowth of phlogopite at temperatures as high as 850 °C. Our two-stage experiments are fully consistent with those two-stage data.

If we were to accept the low-$T$ location of the reaction, as proposed by Peterson and Newton (1989) in their Figure 2, we would be forced to conclude that the (Fl) reaction is located only 30 °C above the fluid-present (Sa) reaction: Phl + Qtz + Fl = En + M. This would represent a surprisingly feeble effect of excess $H_2O$ on the extension of the stability field of melt. Also, if the location of the (Fl) reaction as determined by Peterson and Newton (1989) were correct, then the assemblage phlogopite + quartz would melt at a lower temperature than muscovite + quartz at $P > 1000$ MPa (Storre, 1972; Storre and Karotke, (1972), which seems inconsistent with geological observations.

Furthermore, the existence of a thermal barrier requires the $H_2O$ content of the melt produced by the reaction to be rather low. Our modeling shows that the location of the (F1) curve, as proposed by Peterson and Newton, is actually inconsistent with the existence of a thermal barrier.

## Interpretation and modeling

**Location of the reaction and $H_2O$ activity.** Figure 5 shows the relationship among the $P$-$T$ loci of a simple subsolidus dehydration reaction, the solidus in the system, and the fluid-absent melting reaction as a function of $a_{H_2O}$. The locus of the fluid-absent melting reaction is defined by the intersection of these curves for a given $a_{H_2O}$. Thus, a fluid-absent reaction represents the line along which the invariant point shifts in response to a variation in the activity of $H_2O$. The activity of $H_2O$ changes along the fluid-absent curve, and is uniquely defined at any $P$ and $T$.

Important questions surround how $a_{H_2O}$ varies with increasing pressure, whether it necessarily decreases, and whether there is a minimum beyond which there will be an increase in $a_{H_2O}$. The actual behavior will critically depend on the relative shapes of the solidus and subsolidus curves and their equivalents at reduced activity of $H_2O$.

Case 1: If these curves can be approximated as straight lines, their intersections will produce a fluid-absent reaction along which $a_{H_2O}$ will necessarily decrease with increasing pressure (Fig. 5a). It is clear that there is no equivalent of the reaction H = A + Fl or H + Fl = M for $a_{H_2O} = 0$. Thus, the fluid-absent curve (and more likely its metastable extension) must terminate somewhere, at some very high pressure, where $a_{H_2O}$ is close but not equal to 0.

Case 2: It is common observation that reactions involving $H_2O$, as either a product or reactant, are curved in $P$–$T$ space, concave toward the $P$ axis for the subsolidus curve and its metastable extension, and convex for the solidi. This is caused by the change in the thermodynamic properties of $H_2O$ as a function of $P$ and $T$ and may lead to a situation in which such strongly bending curves intersect twice, generating two invariant points involving the same phases. The fluid-absent curve connects these two points, as shown in Eggler (1973, Fig. 42). The consequence of this situation is that, with increasing pressure, the activity of $H_2O$ along this curve decreases to a minimum value and then increases back to unity at the second, high-pressure, invariant point (Fig. 5b).

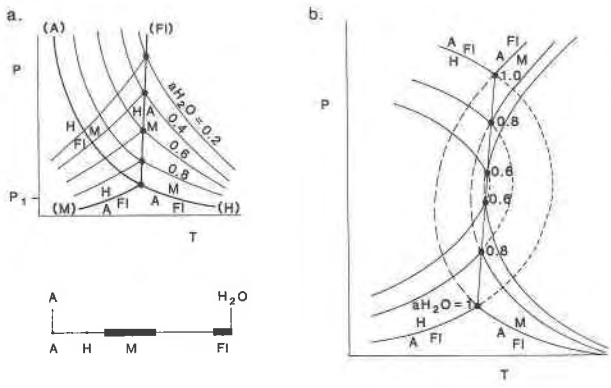


Fig. 5. Topological relationships among the *P-T* loci of a simple subsolidus dehydration reaction, the solidus in the system, and the fluid-absent melting reaction as a function of $a_{H_2O}$. A = an anhydrous crystalline phase, H = a crystalline hydrate, M = the hydrous melt phase of variable composition, and Fl = the supercritical aqueous fluid with some small amount of dissolved component A. (**a**) Their intersection generates a fluid-absent reaction, along which $a_{H_2O}$ decreases with increasing pressure. (**b**) Strongly bending subsolidus and solidus curves intersect twice, generating two invariant points involving the same phases. The fluid-absent curve joins these points. The consequence is that, with increasing pressure, the activity of $H_2O$ along this curve decreases to a minimum and then increases back to unity at the second, higher pressure, invariant point.

Recent calorimetric investigations (Robie and Hemmingway, 1984; Clemens et al., 1987) have yielded thermodynamic data for phlogopite, consistent with the best available experimental results for the subsolidus equilibrium (M): Phl + 3 Qtz = 3 En + Sa + $H_2O$ (Wood, 1976; Bohlen et al., 1983; Peterson and Newton, 1989). Table 4 shows the thermodynamic data (on crystalline phases) used to calculate the *P-T* locus of the reaction Phl + 3 Qtz = 3 En + Sa + $H_2O$. The value quoted for $\Delta G_f^0$ of Al-Si-disordered phlogopite was optimized by taking the high-*T* solution calorimetric data (Clemens et al., 1987) and refining it so as to be fully consistent with the experimental constraints of Wood (1976), as well as with the values for the other phases participating in the reaction. For $H_2O$, the standard-state properties were taken from Robie et al. (1978), whereas the fugacities, at high *P* and *T*, were calculated using functions based on the modified Redlich-Kwong equations of Kerrick and Jacobs (1981), as modified by Perkins et al. (1987). These allow extrapolation of the reaction Phl + 3 Qtz = 3 En + Sa + $H_2O$ (and its metastable extension) to high pressure, using the program Thermo (Perkins et al., 1987). Calculations indicate that the reaction is concave toward the *P* axis and becomes almost parallel to it at $P > 1500$ MPa. The *P-T* locations of the univariant curves for decreasing values of $a_{H_2O}$ down to 0.1 were also calculated by using the relation $\Delta G_{P,T} = -RT\ln a_{H_2O}$ and are shown in Figure 6.

Many experiments are now available on the solidus reaction (En), Phl + Qtz + Sa + $H_2O$ = M (Luth, 1967; Wones and Dodge, 1977; Peterson and Newton, 1989); most of these data are consistent. Peterson and Newton (1989) observed a slope change (from negative to positive) in this solidus reaction, near a pressure of 1000 MPa. This indicates that the fluid-absent reaction we predict from the intersections of the solidus and subsolidus curves can be related to case 2, as described above. The $a_{H_2O}$ along the fluid-absent reaction is expected to first decrease and then increase with increasing pressure.

**Table 4.** Molar thermodynamic data used in calculating the locus of reaction (M): Phl + Qtz = En + Sa + Fl

| Phase | $\Delta G_f^0$ (kJ) | $S^0$ (J/K) | $V^0$ (cm³) |
|---|---|---|---|
| Disordered phlogopite* | | | |
| $KMg_3AlSi_3O_{10}(OH)_2$ | −5838.950 | 334.60 | 149.91 |
| $\beta$ quartz** | | | |
| $SiO_2$ | −856.645 | 30.16 | 23.72 |
| Orthoenstatite† | | | |
| $MgSiO_3$ | −1458.781 | 66.27 | 31.31 |
| High sanidine‡ | | | |
| $KAlSi_3O_8$ | −3739.776 | 232.9 | 109.05 |

* *G*—see text, *S* and $C_P$ equation—Robie and Hemingway (1984), *V*—Robie et al. (1978), thermal expansion—Holland and Powell (1985), compressibility—Birch (1966).

** *G*, *S*, and *V*—extrapolated from $\alpha$ quartz data in Hemingway (1987) and Robie et al. (1978), $C_P$—Hemingway (1987), expansion—Skinner (1966), compressibility—Olinger and Halleck (1976).

† *G*—Brousse et al. (1984), *S*—Krupka et al. (1979), *V*—Danckwerth and Newton (1978), $C_P$—Krupka et al. (1985 a, 1985b), expansion—Skinner (1966), compressibility—Ralph et al. (1981).

‡ *G*, *S*, *V*, and $C_P$—Robie et al. (1978), expansion—Skinner (1966), compressibility—Birch (1966).

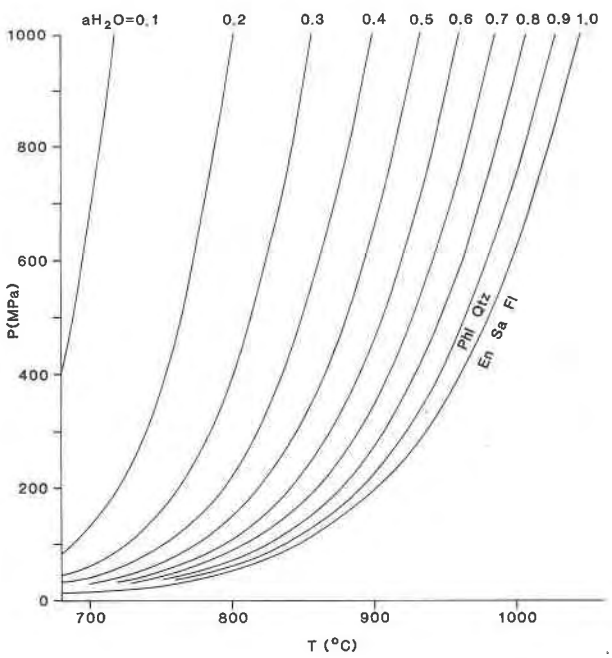


Fig. 6. *P-T* location of the univariant reaction Phl + 3 Qtz = 3 En + Sa + $H_2O$ for various values of $a_{H_2O}$, calculated using the program Thermo (Perkins et al., 1987) and the thermodynamic data in Table 4. Significant portions of these curves are metastable with respect to melting reactions.

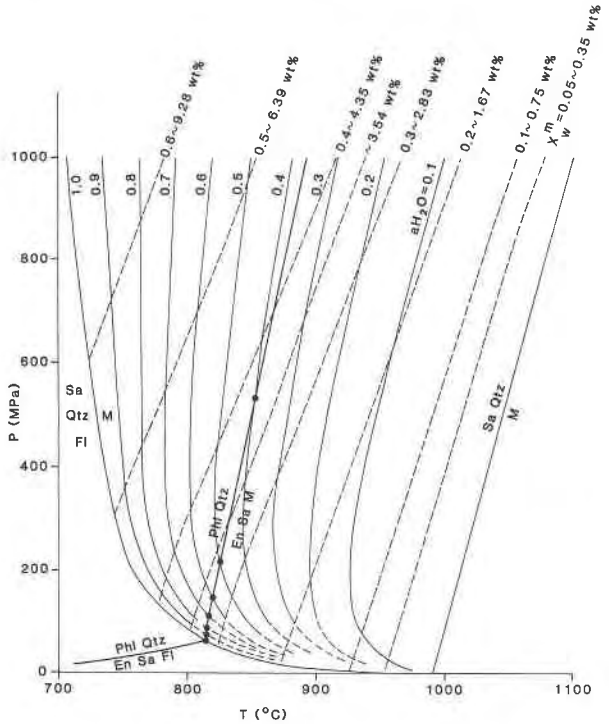


Fig. 7. *P-T* diagram showing the locus of reaction Sa + Qtz + $H_2O$ = M (thin solid lines) as a function of $a_{H_2O}$, as calculated using the computer program of Nekvasil and Burnham (1987), based on a model for aluminosilicate melt-$H_2O$ interactions (Burnham, 1979; Burnham and Nekvasil, 1986). The intersections of these curves with those calculated for the subsolidus reaction (indicated by dots) provide a calculated (theoretical) location for the fluid-absent reaction. Dashed curves represent isopleths of constant $X_{H_2O}$ in the melt ($X_w^M$). The isopleth for 3.54 wt% $H_2O$, corresponding to a limit for the existence of a thermal barrier, is shown also.

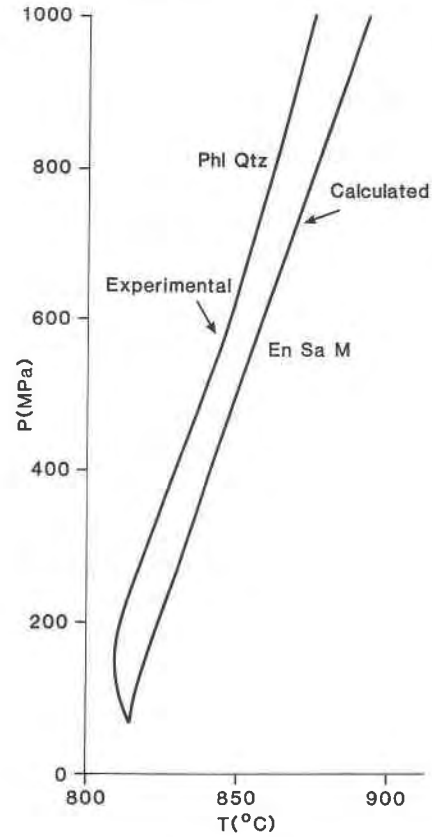


Fig. 8. *P-T* plot showing the relative positions of the experimentally determined and calculated theoretical locus of the fluid-absent melting reaction Phl + Qtz = En + Sa + M.

The determination of thermodynamic constants for the solidus curve is difficult, since it involves a melt whose composition varies with *P* and *T*. However, there is an indirect way of calculating both this curve and its position as a function of $a_{H_2O}$.

In order to extrapolate available experimental data on phase relations in the haplogranite system, Nekvasil and Burnham (1987) produced a computer program based on Burnham's model for aluminosilicate melt-$H_2O$ interactions (Burnham, 1979; Burnham and Nekvasil, 1986). This can be used to predict quantitatively both $H_2O$-saturated and $H_2O$-undersaturated liquidus phase relations in the system and its subsystems. It can be used also to calculate the location of the solidus curves for various values of $a_{H_2O}$.

Due to the very low solubility of MgO in the melt, there is almost no experimentally detectable difference in the *P-T* loci of the reactions

$$\text{Sa} + \text{Qtz} + \text{H}_2\text{O} = \text{M} \quad (1)$$

and

$$\text{Phl} + \text{Sa} + \text{Qtz} + \text{H}_2\text{O} = \text{M} \quad (2)$$

though we know that Reaction 1 is located at a higher *T* than Reaction 2 because, among the phases Sa, Qtz, Fl, and M, MgO (even in small amount) will preferentially enter the melt. Reaction 1 is thus an excellent thermodynamic analogue of Reaction 2. Nekvasil and Burnham's program, with some minor adaptations, allows the calculation of the *P-T* location of Reaction 1 as a function of $a_{H_2O}$ (Fig. 7). The intersections of these curves with those calculated for the subsolidus reaction provide a calculated location for the fluid-absent reaction Phl + Qtz = En + Sa + M (Fig. 7). In Figure 8 the position of this curve is compared with the experimentally determined curve. Note that, up to a pressure of 1000 MPa, the two are in excellent agreement, with a maximum temperature difference of 15 °C.

**Melt $H_2O$ contents and melt proportions.** It is particularly interesting to consider the melting behavior of rocks when a fluid phase composed of pure $H_2O$ exists in the subsolidus region, but in an amount insufficient to saturate the melt at temperatures above the solidus. As an example, consider the partial melting of sanidine plus quartz with 4.3 wt% $H_2O$ ($X_{H_2O}$ = 0.4) at a total pressure of 1000 MPa. This situation is illustrated in the simple isobaric liquidus diagram of Figure 9. Below the solidus, an aqueous fluid will coexist with sanidine and quartz.

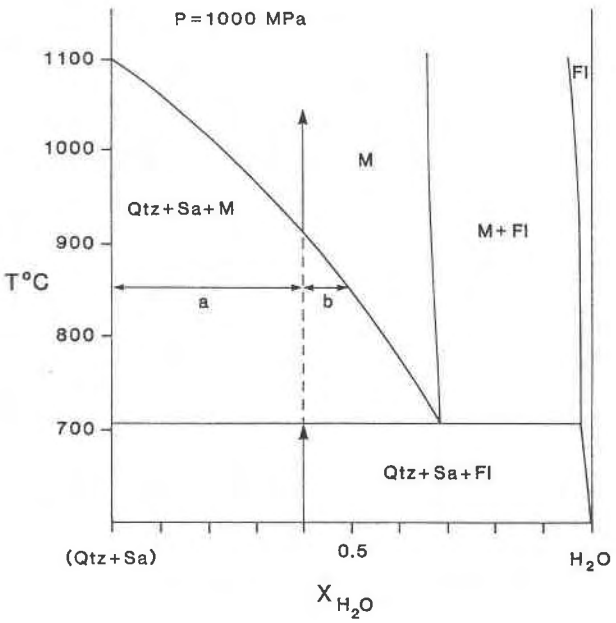


Fig. 9. Pseudobinary liquidus diagram for the system (Qtz + Sa)-$H_2O$ calculated using Burnham's model for aluminosilicate melt-$H_2O$ interactions (Burnham, 1979; Nekvasil and Burnham, 1987). We assume that Qtz and Sa are in the exact proportion so that both phases disappear at the same temperature on the liquidus. Molar proportions can be converted into weight proportions using a molar weight of ~260 for the aluminosilicate component (Qtz + Sa; Qtz considered as $Si_4O_8$). See text for discussion. The boundary of the fluid field is indicative only.

Melting will begin at 707 °C (an isobarically invariant condition), and the first $H_2O$-saturated melt will contain ~12.9 wt% $H_2O$ ($X_{H_2O}$ = 0.68). We assume that $H_2O$ is the limiting factor, i.e., that the amount of melt is not limited by the silicate composition. The amount of melt is thus a simple function of the amount of $H_2O$ in the starting material. At the solidus, the maximum amount of melt will be (wt% $H_2O$ in the system × 100)/(wt% $H_2O$ in melt) = 33.3. The proportion of melt can be estimated graphically in Figure 9 using the lever rule. For this calculation to be valid, Qtz and Sa must be present. At $T$ greater than 707 °C, the composition of the liquid will evolve along the univariant cotectic, where quartz, sanidine, and hydrous melt coexist in the fluid-absent domain. The amount of melt increases with $T$, but the melt will be $H_2O$-undersaturated. If the location of this curve is known, the $H_2O$ content of the melt, and hence its amount, can be determined at any given point. For instance, at $T$ ~854 °C, the $H_2O$ content of the melt along the cotectic is about 6.4 wt% ($X_{H_2O}$ = 0.5), and the amount of melt will be 67.2 wt% [$a/(a + b)$]. At $T$ ~915 °C, the melt will contain 4.3 wt% $H_2O$ ($X_{H_2O}$ = 0.4), which corresponds to the total amount of $H_2O$ in our example, and there will then be 100% melt. This is true only if the silicate composition corresponds exactly to the minimum melt composition for the particular $P$, $T$, and $H_2O$ content (i.e., provided Qtz and Sa disappear at the same temperature). The Nekvasil and Burnham (1987) program allows calculation of the location of any cotectic in the haplogranitic system and its subsystems. Isopleths of constant $X_{H_2O}$ in the melt are shown on the $P$-$T$ projection of Figure 7. These contours may be viewed either as the terminations of the divariant melting intervals for particular $H_2O$ contents in the starting material or as the projections of the Qtz-Sa-M cotectics, such as the one shown in Figure 9, onto the $P$-$T$ plane.

**Table 5.** An equation and its parameters to calculate the $H_2O$ contents of the melts at $P$ and $T$ in the Qtz-Sa-$H_2O$ system for $P \leq 1000$ MPa and $T \leq 1000$ °C

$$\text{Wt\% } H_2O = A_0 + A_P \cdot P\,(\text{MPa}) + A_T \cdot T\,(°\text{C}) + A_{PP} \cdot P^2 + A_{PT} \cdot P \cdot T + A_{TT} \cdot T^2$$

| | Values | ±1σ |
|---|---|---|
| $A_0$ | 53.40 | ±0.60 |
| $A_P$ | $1.692 \cdot 10^{-2}$ | $\pm 2 \cdot 10^{-4}$ |
| $A_T$ | $-9.95 \cdot 10^{-2}$ | $\pm 1.4 \cdot 10^{-3}$ |
| $A_{PP}$ | $1.499 \cdot 10^{-6}$ | $\pm 6.2 \cdot 10^{-8}$ |
| $A_{PT}$ | $-1.644 \cdot 10^{-5}$ | $\pm 2.4 \cdot 10^{-7}$ |
| $A_{TT}$ | $4.607 \cdot 10^{-5}$ | $\pm 7.81 \cdot 10^{-7}$ |

In fluid-absent melting of common crustal rock types, $H_2O$ is usually the factor that limits melt production (i.e., fertility). This can be readily demonstrated by writing the set of linear equations relating the oxide components in a rock to the chemistry of the phases and the bulk composition. Thus, knowledge of the $H_2O$ contents of melts, as a function of $P$ and $T$ in various fluid-absent granitic subsystems, can be used to predict the proportion of melt in various rocks undergoing partial fusion (e.g., Clemens and Vielzeuf, 1987). This method does not work for unusual rocks that are undersaturated in feldspathic components (e.g., Patiño-Douce and Johnston, 1991).

The $H_2O$ contents of the melts in the Qtz-Sa-$H_2O$ system were calculated from the Nekvasil and Burnham (1987) program and fitted to an equation of the form wt% $H_2O = A_o + A_P \cdot P + A_T \cdot T + A_{pp} \cdot P^2 + A_{PT} \cdot P \cdot T + A_{TT} \cdot T^2$ with $P$ in MPa and $T$ in degrees Celsius. Table 5 shows the values of the various constants. This was done using a program of general inversion written by Provost (1989).

Provided that the Qtz-Sa-$H_2O$ system is a reasonable model for the fluid-absent melting of phlogopite + quartz, the foregoing can be used to calculate the values of $a_{H_2O}$, the $H_2O$ content of the melt, and its proportion along the experimentally determined fluid-absent curve. These results are given in Table 6 and shown graphically in Figure

**Table 6.** Calculated $a_{H_2O}$, melt $H_2O$ contents and proportions along the experimentally determined reaction Phl + Qtz= En + Sa + M

| $P$ (MPa) | $T$ (°C) | $a_{H_2O}$ | $X_{H_2O}$ in melt | wt% $H_2O$ in melt | wt% melt |
|---|---|---|---|---|---|
| 1000 | 868 | 0.442 | 0.479 | 5.9 | 37 |
| 800 | 861 | 0.425 | 0.436 | 5.1 | 42 |
| 600 | 847 | 0.435 | 0.408 | 4.5 | 48 |
| 400 | 829 | 0.480 | 0.379 | 4.1 | 53 |
| 200 | 812 | 0.590 | 0.353 | 3.8 | 57 |
| 100 | 812 | 0.795 | 0.336 | 3.4 | 64 |

*Note:* The proportion of melt was calculated considering a $H_2O$ content of 2.16 wt% in the starting material.

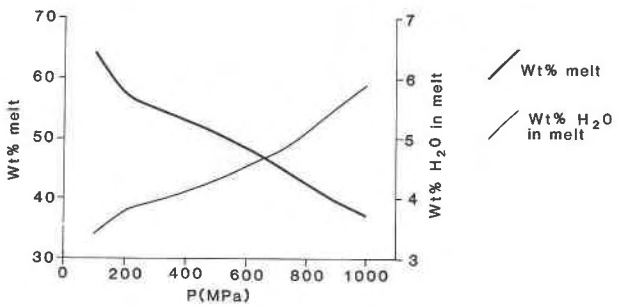


Fig. 10. Calculated melt $H_2O$ contents and proportions along the experimentally determined reaction Phl + Qtz = En + Sa + M. The proportion of melt was calculated on the basis that the starting material contains 2.16 wt% $H_2O$.

10. The activity of $H_2O$ decreases from 1 at the invariant point to 0.4 at 800 MPa. Thereafter, it increases very slowly, as predicted earlier. The calculated $H_2O$ content of the melt varies from 3.3 wt% at 100 MPa to 5.8 wt% at 1000 MPa. Since the $H_2O$ content of the starting material is about 2.16 wt%, the amount of melt will decrease from about 64% at 100 MPa to about 37% at 1000 MPa. These figures correspond to a situation where phlogopite is entirely consumed in the melting reaction, which is not the case in most of our experiments at $T \leq 910$ °C, probably because of the poor kinetics of the reaction. Note that the Sa-Qtz-$H_2O$ subsystem cannot be used to predict the amounts of melt formed from most rock systems because plagioclase is not taken into consideration. This subsystem can be used only for rocks containing quartz, biotite, and potassium feldspar as the sole major phases.

**Singular points and thermal barrier.** The potential existence of two singular points on the (Fl) curve is directly connected to the variation of the $H_2O$ content of the melt as a function of pressure (Eggler, 1973; Grant, 1986). Wyllie and Tuttle (1959) described the occurrence of such points and associated "reactions of restricted univariance" in systems where volatile solubilities in melts vary as a function of $P$. This early description is exactly analogous to the present occurrence in KMASH. At the invariant point, located at around 815 °C and 65 MPa, the melt will have a $H_2O$ content of about 3.1 wt% and, as pointed out by Grant (1986), plots to the left of the Phl-En tie line in Figure 1d. Grant (1986) calculated that an anhydrous equivalent of the eutectic melt, plotting at $X_{H_2O} = 0.5$ and $X_{KAlO_2} = 0.5$ (on the extension of the Phl-En tie Line), would have to contain 3.5 wt% $H_2O$. With a liquid composition of $SiO_2 = 79.50$, $Al_2O_3 = 10.38$, MgO = 0.52, and $K_2O = 9.59$ wt% [corresponding to 57 wt% Sa and 43 wt% Qtz (Luth, 1976) plus a minor amount of MgO], the fluid-absent reaction will switch from Phl + Sa + Qtz = En + M to Phl + Qtz = En + Sa + M, at a melt $H_2O$ content of 3.54%, entirely in agreement with Grant (1986). A first singular point ($S_1$) and a thermal barrier (Phl + Qtz = M + En) are created when the point corresponding to the composition of the liquid formed in reaction (Sa) migrates across the Phl-En tie line in Figure 1d, as a result of increasing pressure. There, the $H_2O$ content of the melt should be very close to 3.5 wt%. The thermal barrier terminates at the pressure where the point representing the melt formed by the (Fl) reaction intersects the extension of the Phl-En tie line. There, the $H_2O$ content of the melt will be slightly greater than 3.5 wt%. There seems little reason to suspect that the critical value of 3.54 wt% would change significantly with increasing pressure, particularly since little MgO is dissolved in the melt. Thus, we believe that a value close to 3.54 wt% $H_2O$ in the melt represents the limit beyond which singular points will not exist. In other words, this represents a pressure constraint on the location of a thermal barrier. An isopleth corresponding to 3.54 wt% in the melt is shown on the $P$-$T$ diagram of Figure 7. This line separates $P$-$T$ regions in which the melt $H_2O$ contents are greater or less than 3.54. When considered in conjunction with the various experimental determinations of the fluid-absent reaction, two results appear: (1) The results of Bohlen et al. (1983) are consistent with a thermal barrier terminating somewhere between 350 and 400 MPa, at about 830–850 °C. This is very close to the location of $S_2$, as proposed by Grant (1986). (2) All the other data sets (Peterson and Newton, 1989; Montana and Brearley, 1989; this study) indicate that singular points and the thermal barrier cannot exist above about 100–150 MPa at $T \sim 810$ °C. This is inconsistent with the observations and interpretations of Peterson and Newton, who postulated the existence of a thermal barrier at about 815 °C, extending to pressures as high as 2000 MPa (their Fig. 2). Note that at 1000 MPa and 816 °C, where these authors locate the (Fl) reaction, the melt $H_2O$ content is 7.9 wt%. Such a melt cannot lie on the extension of the En-Phl tie line.

How should we interpret the apparent scarcity of sanidine in the experimental products? First, our experiments certainly produced sanidine at 100, 150, 1000, and 1500 MPa. We believe that sanidine is not commonly observed because the first melt formed at reaction (Fl) must be rather close to the extension of the En-Phl tie line, though on the $H_2O$ side. The temperature interval over which En, Sa, and M may coexist along the cotectic is thus severely limited (see Fig. 1d at $P_3$). Bohlen et al. (1983) may have observed sanidine at very high temperatures because of its metastable persistence in the short-duration experiments.

Although the model for the solubility of $H_2O$ in aluminosilicate melts, on which the preceding calculations are based, may be open to contention, we believe that it provides a basis for useful discussion, in the absence of definitive experiments. As a consequence, we suggest that the singularities mooted by Grant (1986) may well exist but must be restricted to a very narrow domain between 65 and 100 MPa, at about 810 °C. They would imply a topology such as that presented in Figure 4, with $S_1$ and $S_2$ located at about the same temperature as the invariant point.

Available experimental data (Forbes and Flowers, 1974; Robert, 1976; Tronnes et al., 1985) indicate that the phlogopite + quartz melting equilibria will be shifted to higher temperatures with the addition of $Ti^{4+}$ to the system (see Peterson and Newton, 1989, p. 481 for a detailed discussion). This would have the effect of significantly extending the thermal barrier. The same reasoning applies for F (Peterson et al., 1991). A shift of 60 °C in the fluid-absent curve, toward higher temperatures, would result in the extension of the thermal barrier to about 800–900 MPa, provided the $dP/dT$ reaction slope and the $H_2O$ contents of the melts were not significantly modified by the addition of Ti or F to the system. This would render Grant's (1986) theoretical considerations particularly relevant.

## Conclusion

In agreement with the McKenna and Hodges (1988) statement on the accuracy vs. precision in $P$-$T$ curve locations, "we feel that arguments such as 'the reaction has been calibrated already' are not sufficient reasons to avoid repeating experiments. The operative questions must be 'how well should we know this reaction?' and 'how many brackets will that require?'" It seems that the fluid-absent phlogopite-quartz reaction, in spite of its apparent simplicity, is one of those requiring many complementary experiments to settle the question of its location and character.

## Acknowledgments

This study was begun while J.D.C. was Directeur de Recherche Associé at Clermont-Ferrand for two years. Funding for this study was provided principally through Université Blaise Pascal and Centre National de la Recherche Scientifique (France). Experimental work was supported by CNRS-INSU through contracts 91 DBT 3.28 and 91 DBT 4.09 to D.V. Part of J.D.C.'s contribution to this research was funded through the Natural Environment Research Council (U.K.) grant GR3/7669. The final stage of the program benefitted from a NATO collaborative research grant to D.V. We are grateful to Y. Blanc and M. Veschambre for their help in XRD and microprobe analyses and to J.A. Grant and J.W. Peterson for outstandingly rigorous reviews, which helped us in clarifying our views and interpretations. Figures were drafted by R.S. Hartley and photo processing was by M.S. Maher, both at Manchester. This is contribution CNRS-INSU-DBT no. 431, thème "Fluides, Minéraux et Cinétique."

## References cited

Akella, J., and Kennedy, G.C. (1971) Melting of gold, silver, and copper—Proposal for a new high-pressure calibration scale. Journal of Geophysical Research, 76, 4969–4977.

Birch, F. (1966) Compressibility: Elastic constants. In S.P. Clark, Jr., Ed., Handbook of physical constants. Geological Society of America Memoir, 97, 97–174.

Bohlen, S.R. (1984) Equilibria for precise pressure calibration and a frictionless furnace assembly for the piston cylinder apparatus. Neues Jahrbuch für Mineralogie Monatshefte, H9, 404–412.

Bohlen, S.R., and Boettcher, A.L. (1982) The quartz ↔ coesite transformation: A precise determination and the effects of other components. Journal of Geophysical Research, 87, 7073–7078.

Bohlen, S.R., Boettcher, A.L., Wall, V.J., and Clemens, J.D. (1983) Stability of phlogopite-quartz and sanidine-quartz. A model for melting in the lower crust. Contributions to Mineralogy and Petrology, 83, 270–277.

Brousse, C., Newton, R.C., and Kleppa, O.J. (1984) Enthalpy of formation of forsterite, enstatite, akermanite, monticellite and merwinite at 1073 K determined by alkali borate solution calorimetry. Geochimica et Cosmochimica Acta, 48, 1081–1088.

Burnham, C.W. (1979) The importance of volatile constituents. In H.S. Yoder, Ed., The evolution of the igneous rocks (Fiftieth anniversary perspectives), p. 439–482. Princeton University Press, Princeton, New Jersey.

Burnham, C.W., and Nekvasil, H. (1986) Equilibrium properties of granite pegmatite magmas. American Mineralogist, 71, 239–263.

Cemic, L., Geiger, C.A., Hoger, W.W., Koch-Müller, M., and Langer, K. (1990) Piston cylinder techniques: Pressure and temperature calibration of a pyrophyllite-based assembly by means of DTA measurements, a salt-based assembly, and a cold sealing sample encapsulating method. Neues Jahrbuch für Mineralogie Monatshefte, H2, 49–64.

Clemens, J.D., and Vielzeuf, D. (1987) Constraints on melting and magma production in the crust. Earth and Planetary Science Letters, 86, 287–306.

Clemens, J.D., and Wall, V.J. (1981) Crystallization and origin of some peraluminous (S-type) granitic magmas. Canadian Mineralogist, 19, 111–132.

Clemens, J.D., Circone, S., Navrotsky, A., McMillan, P.F., Smith, B.K., and Wall, V.J. (1987) Phlogopite: High temperature solution calorimetry, thermodynamic properties. Al-Si and stacking disorder, and phase equilibria. Geochimica et Cosmochimica Acta, 51, 2569–2578.

Danckwerth, P.A., and Newton, R.C. (1978) Experimental determination of the spinel peridotite to garnet peridotite reaction in the system MgO-$Al_2O_3$-$SiO_2$ in the range 900–1100 °C and $Al_2O_3$ isopleths of enstatite in the spinel field. Contributions to Mineralogy and Petrology, 66, 189–201.

Eggler, D.H. (1973) Principles of melting of hydrous phases in silicate melt. Carnegie Institution of Washington Year Book, 72, 491–495.

Eggler, D.H., and Holloway, J.R. (1977) Partial melting of peridotite in the presence of $H_2O$ and $CO_2$: Principles and review. Magma Genesis, Oregon Department of Geology and Mineral Industries Bulletin, 96, 15–36.

Esperança, S., and Holloway, J.R. (1986) The origin of the high-K latites from Camp Creek, Arizona: Constraints from experiments with variable $f_{O_2}$ and $a_{H_2O}$. Contributions to Mineralogy and Petrology, 93, 504–512.

Forbes, W.C., and Flowers, M.F.J. (1974) Phase relations of titan-phlogopite, $K_2Mg_4TiAl_2Si_6O_{20}(OH)_4$: A refractory phase in the upper mantle? Earth and Planetary Science Letters, 22, 60–66.

Fyfe, W.S. (1973) The granulite facies, partial melting and the Archean crust. Philosophical Transactions of the Royal Society of London, A273, 451–461.

Grant, J.A. (1973) Phase equilibria in high grade metamorphism and partial melting of pelitic rocks. American Journal of Science, 273, 289–317.

——— (1986) Quartz-phlogopite-liquid equilibria and origins of charnockites. American Mineralogist, 71, 1071–1075.

Hemingway, B.S. (1987) Quartz: Heat capacities from 340 to 1000 K and revised values of the thermodynamic properties. American Mineralogist, 72, 273–279.

Hewitt, D.A., and Wones, D.R. (1975) Physical properties of some synthetic Fe-Mg-Al trioctahedral biotites. American Mineralogist, 60, 854–862.

Holland, T.J.B., and Powell, R. (1985) An internally consistent thermodynamic data set with uncertainties and correlations: 2—Data and results. Journal of Metamorphic Geology, 3, 343–370.

Jakobsson, S., and Holloway, J.R. (1986) Crystal-liquid experiments in the presence of a C-O-H fluid buffered by graphite + iron + wustite: experimental method and near-liquidus relations in basanite. Journal of Volcanology and Geothermal Research, 29, 265–291.

Kerrick, D.M., and Jacobs, G.K. (1981) A modified Redlich-Kwong equation for $H_2O$, $CO_2$, and $H_2O$-$CO_2$ mixtures at elevated pressures and temperatures. American Journal of Science, 281, 736–767.

Krupka, K.M., Kerrick, D.M., and Robie, R.A. (1979) Heat capacities of synthetic orthoenstatite and natural anthophyllite from 5 to 1000 K. Eos, 60, 405.

Krupka, K.M., Hemingway, B.S., Robie, R.A., and Kerrick, D.M. (1985a)

High-temperature heat capacities and derived thermodynamic properties of anthophyllite, diopside, dolomite, enstatite, bronzite, talc, tremolite and wollastonite. American Mineralogist, 70, 261–271.

Krupka, K.M., Robie, R.A., Hemingway, B.S., and Kerrick, D.M. (1985b) Low-temperature heat capacities and derived thermodynamic properties of anthophyllite, diopside, enstatite, bronzite, and wollastonite. American Mineralogist, 70, 249–260.

Luth, W.C. (1967) Studies in the system $KAlSiO_4$-$Mg_2SiO_4$-$SiO_2$-$H_2O$: I, Inferred phase relations and petrologic application. Journal of Petrology, 8, 372–416.

——— (1976) Granitic rocks, In D.K. Bailey and R. Macdonald, Eds., The evolution of the crystalline rocks, p. 335–417. Academic Press, New York.

McKenna, L.W., and Hodges, K.V. (1988) Accuracy versus precision in locating reaction boundaries: Implications for the garnet–plagioclase–aluminum silicate–quartz geobarometer. American Mineralogist, 73, 1205–1208.

Montana, A., and Brearley, M. (1989) An appraisal of the stability of phlogopite in the crust and the mantle. American Mineralogist, 74, 1–4.

Nekvasil, H. (1988) Calculated effect of anorthite component on the crystallization paths of $H_2O$-undersaturated haplogranitic melts. American Mineralogist, 73, 966–981.

Nekvasil, H., and Burnham, C.W. (1987) The calculated individual effects of pressure and water content on phase equilibria in the granite system. In B.O. Mysen, Ed., Magmatic processes: Physiochemical principles. Geochemical Society Special Publication, 1, 433–445.

Nicholls, I.A. (1974) A direct fusion method of preparing rock glasses for energy-dispersive electron microprobe analysis. Chemical Geology, 14, 151–157.

Olinger, B., and Halleck, P.M. (1976) The compression of alpha quartz. American Mineralogist, 67, 203–222.

Patera, E.S., and Holloway, J.R. (1982) Experimental determination of the spinel-garnet boundary in a Martian mantle composition. Journal of Geophysical Research , 87 (suppl.), A31–A36.

Patiño-Douce, A.E., and Johnston, A.D. (1991) Phase equilibria and melt productivity in the pelitic system: Implications for the origin of peraluminous granitoids and aluminous granulites. Contributions to Mineralogy and Petrology, 107, 202–218.

Perkins, D., and Vielzeuf, D. (1992) Reinvestigation of fayalite + anorthite = garnet. Contributions to Mineralogy and Petrology, in press.

Perkins, D., III, Holland, T.J.B., and Newton, R.C. (1981) The $Al_2O_3$ contents of enstatite in equilibrium with garnet in the system MgO-$Al_2O_3$-$SiO_2$ at 15–40 kbar and 900–1600 °C. Contributions to Mineralogy and Petrology, 78, 99–109.

Perkins, D., Essene, E.J., and Wall, V.J. (1987) Thermo: A computer program for calculation of mixed-volatile equilibria. American Mineralogist, 72, 446–447.

Peterson, J.W., and Newton, R.C. (1988) Experimental constraints on the vapor-absent melting of phlogopite + quartz. Eos, 69, 498.

——— (1989) Reversed experiments on biotite-quartz-feldspar melting in the KMASH: Implications for crustal anatexis. Journal of Geology, 97, 465–485.

Peterson, J.W., Chacko, T., and Kuehner, S.M. (1991) The effects of fluorine on the vapor-absent melting of phlogopite + quartz: Implications for deep-crustal processes. American Mineralogist, 76, 470–476.

Provost, A. (1989) Block-wise global inversion. Terra Abstracts, 1, 328.

Ralph, R.L., Hazen, R.M., and Finger, L.W. (1981) Cell parameters of orthoenstatite at high temperature and pressure. Carnegie Institution of Washington Year Book, 80, 376–379.

Robert, J.L. (1976) Phlogopite solid solutions in the system $K_2O$-MgO-$Al_2O_3$-$SiO_2$-$H_2O$. Chemical Geology, 17, 195–212.

Robertson, J.K., and Wyllie, P.J. (1971) Rock-water systems with special reference to the water-deficient region. American Journal of Science, 271, 252–277.

Robie, R. A., and Hemingway, B.S. (1984) Heat capacities and entropies of phlogopite ($KMg_3[AlSi_3O_{10}](OH)_2$) and paragonite ($NaAl_2[AlSi_3O_{10}](OH)_2$) between 5 and 900 K and estimates of the enthalpies and Gibbs free energies of formation. American Mineralogist, 69, 858–868.

Robie, R.A., Hemingway, B.S., and Fisher, J.R. (1978) Thermodynamic properties of minerals and related substances at 298.15 K and 1 bar ($10^5$ Pascals) pressure and at higher temperatures. U.S. Geological Survey Bulletin, 1452, 456 p.

Skinner, B.J. (1966) Thermal expansion. Geological Society of America Memoir, 97, 75–96.

Storre, B. (1972) Dry melting of muscovite + quartz in the range Ps = 7 kb to Ps = 20 kb. Contributions to Mineralogy and Petrology, 37, 87–89.

Storre, B., and Karotke, E. (1972) Experimental data on melting reactions of muscovite + quartz in the system $K_2O$-$Al_2O_3$-$SiO_2$-$H_2O$ to 20 kb water pressure. Contributions to Mineralogy and Petrology, 36, 343–345.

Tronnes, R.G., Edgar, A.D., and Arima, M. (1985) A high pressure–high temperature study of $TiO_2$ solubility in Mg-rich phlogopite: Implications to phlogopite chemistry. Geochimica et Cosmochimica Acta, 49, 2323–2329.

Wones, D.R. (1963) Physical properties of synthetic biotites on the join phlogopite-annite. American Mineralogist, 48, 1300–1321.

——— (1967) A low pressure investigation of the stability of phlogopite. Geochimica et Cosmochimica Acta, 31, 2248–2253.

Wones, D.R., and Dodge, F.C.W. (1977) The stability of phlogopite in the presence of quartz and diopside. In D.G. Fraser, Ed., Thermodynamics in geology, p. 229–247. D. Reidel, Dordrecht, the Netherlands.

Wood, B.J. (1976) The reaction phlogopite + quartz = enstatite + sanidine + $H_2O$. Progress in Experimental Petrology, 6, 17–19.

Wright, T.L. (1968) X-ray and optical study of alkali feldspar: II. An X-ray method for determining the composition and structural state from measurement of $2\theta$ values from three reflections. American Mineralogist, 53, 88–104.

Wyllie, P.J., and Tuttle, O.F. (1959) Effect of carbon dioxide on the melting of granites and feldspars. American Journal of Science, 257, 648–655.

Yoder, H.S., and Eugster, H.P. (1954) Phlogopite synthesis and stability range. Geochimica et Cosmochimica Acta, 6, 157–185.

Yoder, H.S., Jr., and Kushiro, I. (1969) Melting of a hydrous phase: Phlogopite. American Journal of Science, 267A, 558–582.

Manuscript received July 18, 1991
Manuscript accepted July 17, 1992